Published in final edited form as:

Bioconjug Chem. 2009 December ; 20(12): 2199–2213. doi:10.1021/bc900167c.

Radiolabeled Cyclic RGD Peptides as Integrin $\alpha_v\beta_3$-Targeted Radiotracers: Maximizing Binding Affinity via Bivalency

Shuang Liu

School of Health Sciences, Purdue University, 550 Stadium Mall Drive, West Lafayette, IN 47907, Phone: 765-494-0236 and Email: lius@pharmacy.purdue.edu

Abstract

Integrin $\alpha_v\beta_3$ plays a significant role in tumor angiogenesis, and is a receptor for the extracellular matrix proteins with the exposed arginine-glycine-aspartic (RGD) tripeptide sequence. These include vitronectin, fibronectin, fibrinogen, lamin, collagen, Von Willibrand's factor, osteoponin, and adenovirus particles. Integrin $\alpha_v\beta_3$ is expressed at low levels on epithelial cells and mature endothelial cells, but it is overexpressed on the activated endothelial cells of tumor neovasculature and some tumor cells. The restricted expression of integrin $\alpha_v\beta_3$ during tumor growth, invasion and metastasis present an interesting molecular target for both early detection and treatment of rapidly growing solid tumors. Over the last decade, many radiolabeled linear and cyclic RGD peptide antagonists have been evaluated as the integrin $\alpha_v\beta_3$-targeted radiotracers. Significant progress has been made on their use for imaging integrin $\alpha_v\beta_3$-positive tumors by SPECT or PET. Among the radiotracers evaluated in pre-clinical tumor-bearing models, [^{18}F]Galacto-RGD (2-[^{18}F]fluoropropanamide c(RGDfK (SAA); SAA = 7-amino-L-glyero-L-galacto-2,6-anhydro-7-deoxyheptanamide) and [^{18}F]-AH111585 are currently under clinical investigation for visualization of integrin $\alpha_v\beta_3$ expression in cancer patients. However, their low tumor uptake, high cost and lack of preparative modules for routine radiosynthesis will limit their continued clinical applications. Thus, there is a continuing need for more efficient integrin $\alpha_v\beta_3$-targeted radiotracers that are readily prepared from a kit formulation without further post-labeling purification. This article will focus on different approaches to maximize the targeting capability of cyclic RGD peptides and to improve the radiotracer excretion kinetics from non-cancerous organs. Improvement of tumor uptake and tumor-to-background ratios is important for early detection of integrin $\alpha_v\beta_3$-positive tumors and/or noninvasive monitoring of therapeutic efficacy of antiangiogenic therapy.

Keywords

Integrin $\alpha_v\beta_3$; PET and SPECT radiotracers; tumor imaging

Introduction

Cancer is the second leading cause of death worldwide. Although the exact cause of cancer remains unknown, most cancer patients will survive after surgery, radiation therapy, and chemotherapy or a combination thereof if it can be detected at the early stage. Thus, accurate early detection is highly desirable so that appropriate therapy can be given before the primary tumors become widely spread.

Tumors produce many angiogenic factors, which are able to activate endothelial cells in established blood vessels and induce endothelial proliferation, migration, and new vessel formation (angiogenesis) through a series of sequential but partially overlapping steps. Angiogenesis is a requirement for tumor growth and metastasis (1–7). Without the neovasculature to provide oxygen and nutrients, tumors cannot grow beyond 1–2 mm in size.

Once vascularized, the tumors begin to grow rapidly. The angiogenic process depends on vascular endothelial cell migration and invasion, is regulated by cell adhesion receptors. Integrins are such a family of proteins that facilitate the cellular adhesion to and the migration on extracellular matrix proteins in the intercellular spaces and basement membranes, and regulate cellular entry and withdraw from the cell cycle (7–10). Integrin $\alpha_v\beta_3$ serves as a receptor for extracellular matrix proteins with exposed arginine-glycine-aspartic (RGD) tripeptide sequence (8–13). These include vitronectin, fibronectin, fibrinogen, lamin, collagen, osteoponin and adenovirus particles. Integrin $\alpha_v\beta_3$ is expressed at low levels on epithelial cells and mature endothelial cells; but it is highly expressed on activated endothelial cells in neovasculature of tumors, including osteosarcomas, neuroblastomas, glioblastomas, melanomas, lung carcinomas and breast cancer (14–16). It has been demonstrated that integrin $\alpha_v\beta_3$ is overexpressed on both the endothelial cells and tumor cells in human breast cancer xenografts (17). The integrin $\alpha_v\beta_3$ expression correlates well with tumor progression and invasiveness of melanoma, glioma, ovarian and breast cancers (10–17). The restricted expression of integrin $\alpha_v\beta_3$ during tumor growth, invasion and metastasis present an interesting molecular target for diagnosis and treatment of the rapidly growing and metastatic tumors (18–32).

Over the last decade, many radiolabeled cyclic RGD peptides have been evaluated as radiotracers for imaging tumors by SPECT or PET (33–68). Several review articles have appeared covering the nuclear medicine applications of radiolabeled cyclic RGD peptide and non-peptide antagonists as radiotracers for diagnosis and radiotherapy of integrin $\alpha_v\beta_3$–positive tumors (17–29). This article is not intended to be an exhaustive review of the current literature on radiolabeled RGD peptides and nuclear medicine applications. Instead, it will focus on different approaches to maximize their targeting capability and to improve the radiotracer excretion kinetics from non-cancerous organs. Improvement of tumor uptake and tumor-to-background (T/B) ratios is important for both diagnostic and therapeutic radiotracers.

Radiotracer Design

Figure 1 shows a schematic illustration of an integrin $\alpha_v\beta_3$-targeted radiotracer. Cyclic RGD peptide serves as the targeting biomolecule to carry radionuclide to the integrin $\alpha_v\beta_3$ overexpressed on tumor cells and activated endothelial cells of tumor neovasculature. A multidentate bifunctional chelator (BFC) is used to attach the metallic radionuclide to the cyclic RGD peptide (69–72), whereas an organic precursor or synthon is often needed for the ^{18}F-labeling (73). The pharmacokinetic modifying linker (PKM) is used to improve the radiotracer excretion kinetics (69–71). For a new integrin $\alpha_v\beta_3$-targeted radiotracer to be successful, it must show clinical indications for high-incidence tumors (breast, lung, colorectal, prostate and skin cancers). The radiotracer should have high tumor uptake and T/B ratios in a short period of time. To achieve this goal, the radiotracer should have a rapid blood clearance to minimize background radioactivity. Since most high-incidence tumors (breast, lung and colorectal cancers) occur in the torso, renal excretion is necessary to avoid radioactivity accumulation in the gastrointestinal tract. The integrin $\alpha_v\beta_3$-targeted radiotracer should also be able to distinguish between benign and malignant tumors, to follow tumor growth and metastasis, and to predict therapeutic efficacy in integrin $\alpha_v\beta_3$-positive cancer patient. In addition, a kit formulation or preparative module is needed for routine preparation of the radiotracer in high yield and radiochemical purity at low cost.

Choice of Radionuclide

The choice of radionuclide depends largely on the clinical utility of radiotracer. For planar imaging and SPECT, more than 80% of radiotracers used in nuclear medicine departments are ^{99m}Tc compounds due to optimal nuclear properties of ^{99m}Tc and its easy availability at

low cost (69–72). The 6 h half-life is long enough to allow radiopharmacists to carry out radiosynthesis and for physicians to collect clinically useful images. At the same time, it is short enough to permit administration of 20–30 mCi of ^{99m}Tc without imposing a significant radiation dose to the patient. The monochromatic 140 KeV photons are readily collimated to give high quality images with high spatial resolution. The clinically most relevant radionuclides for PET include ^{18}F, ^{62}Cu, ^{64}Cu and ^{68}Ga.

^{18}F is a cyclotron-produced isotope suitable for PET. It has a half-life of 110 min. For several years, ^{18}F-FDG (FDG = 2-fluoro-2-deoxyglucose) has been widely used as an imaging tool for diagnosis of cancers, brain and cardiovascular diseases. Despite its short half-life, the availability of preparative modules makes ^{18}F-labeled biomolecules much more accessible to researchers and clinicians in many clinical institutions.

^{62}Cu is a generator-produced radionuclide from the decay of ^{62}Zn. Its 9.7 min half-life allows repeated dosing without imposing a significant radiation burden to the patient. The commercially available ^{62}Zn-^{62}Cu generator has been successfully used in clinical trials (74–77). ^{64}Cu is another PET isotope useful for development of target-specific radiotracers. It has a half-life of 12.7 h and a β^+ emission (18%, E_{max} = 0.655 MeV). Despite poor nuclear properties, its long half-life makes it feasible to prepare, transport, and deliver the ^{64}Cu radiotracer for clinical applications. More importantly, recent breakthroughs in production of ^{64}Cu with high specific activity have made it more available to the small research institutions without on-site cyclotron facilities (78). ^{64}Cu is a viable alternative to ^{18}F for research programs that wish to incorporate high sensitivity and high spatial resolution of PET, but cannot afford to maintain the expensive radionuclide production infrastructure. Copper radionuclides and related radiochemistry have been reviewed by Blower et al (79). Nuclear medicine applications of ^{64}Cu-labeled monoclonal antibodies and peptides have been reviewed by Anderson et al (75,80).

^{68}Ga is generator-produced PET isotope with a half-life of 68 min. The ^{68}Ge-^{68}Ga generator can be used for more than a year, allowing PET studies without the on-site cyclotron. If the radiotracer is properly designed, ^{68}Ga could become as useful for PET as ^{99m}Tc for SPECT (81,82). In support of this, the ^{68}Ga-labeled somatostatin analogs have been studied extensively for PET imaging of somatostatin-positive tumors in animal models and cancer patients (83–91). Gallium chemistry and related medical applications have been reviewed recently (81,82, 92).

Bifunctional Chelators

The choice of BFC depends on the radionuclide. ^{18}F can be incorporated into the cyclic RGD peptide via a covalent bond without the need for BFC. In contrast, BFC is an important part of radiotracers containing a metallic radionuclide (69–72,92). Among various BFCs (Figure 2), 6-hydazinonicotinic acid (HYNIC) is of great interest due to its high ^{99m}Tc-labeling efficiency (rapid radiolabeling and high radiolabeling yield), the high solution stability of its ^{99m}Tc complexes, and the easy use of different coligands for modification of biodistribution characteristic of ^{99m}Tc-labeled small biomolecules (93). DOTA (1,4,7,10-tetraazacyclododecane-1,4,7,10-tetraacetic acid), NOTA (1,4,7-tritazacyclononane-1,4,7-triacetic acid) and their derivatives (Figure 2) have been used as BFCs for ^{68}Ga and ^{64}Cu-labeling small biomolecules (84–91). NODAGA is particularly useful for ^{68}Ga- and ^{64}Cu-labeling due to high hydrophilicity and in vivo stability of its ^{68}Ga and ^{64}Cu chelates. It has been reported that NOTA derivatives have much higher ^{68}Ga and ^{64}Cu-labeling efficiency than their DOTA analogs (94–98). The fast and efficient radiolabeling is especially critical for ^{68}Ga and ^{62}Cu due to their short half-life ($t_{1/2}$ = 68 min for ^{68}Ga and 9.7 min for ^{62}Cu).

PKM Linkers

In general, high lipophilicity often leads to more hepatobiliary excretion and/or high protein binding, which will results in longer blood retention of radioactivity. Hepatobiliary excretion is detrimental for improvement of T/B ratio. Thus, an important aspect of radiotracer development is to improve T/B ratios by modifying pharmacokinetics of radiolabeled cyclic RGD peptides. For example, the negatively charged small peptide sequences or amino acids have been proposed as PKM linkers to reduce renal uptake and kidney retention of radiolabeled small biomolecules (70,71,92). The di(cysteic acid) linker has successfully been used to improve the blood clearance and minimize the liver and kidney activity of radiolabeled nonpeptide integrin $\alpha_v\beta_3$ receptor antagonists (99–102). The Asp_3 and Ser_3 tripeptide sequences were also used to modify excretion kinetics of the ^{99m}Tc-labeled cyclic RGD peptide (39). Harris et al reported the use of a PEG_4 (15-amino-4,7,10,13-tetraoxapentadecanoic acid) linker to improve the tumor uptake and T/B ratios of the ^{99m}Tc-labeled nonpeptide integrin $\alpha_v\beta_3$ receptor antagonists (99–102). Kessler et al reported the use of HEG (hexaethylene glycolic acid) as the PKM linker for the ^{18}F-labeled cyclic RGDfE dimers and tetramers (40–42). Using the HEG linker also increases the distance between the cyclic RGD motifs. Chen et al also found that the introduction of the PEG (polyethylene glycolic acid) linker can improve the tumor uptake and excretion kinetics of ^{125}I- and ^{18}F-labeled c(RGDyK) and ^{64}Cu-labeled $E[c(RGDyK)]_2$ (48,49,54,103).

Targeting Biomolecules

Figure 3 shows several examples of cyclic RGD peptides that have high affinity and selectivity for integrin $\alpha_v\beta_3$. Among the radiotracers evaluated in pre-clinical tumor-bearing models, [^{18}F]Galacto-RGD (Figure 3: 2-[^{18}F]fluoropropanamide c(RGDfK(SAA); SAA = 7-amino-L-glyero-L-galacto-2,6-anhydro-7-deoxyheptanamide) and [^{18}F]-AH111585, the core sequence of which was originally discovered from a phage display library (as ACDRGDCFCG), are currently under clinical investigation for visualization of integrin $\alpha_v\beta_3$ expression in cancer patients (104–109). The results from imaging studies in cancer patients show that there is sufficient integrin $\alpha_v\beta_3$ expression for PET imaging, and the accumulation of radiolabeled RGD peptide radiotracer correlates well with the integrin $\alpha_v\beta_3$ expression levels in cancer patients (108,109). However, their relatively low tumor uptake, the high cost and lack of preparative modules for routine radiosynthesis will limit their continued clinical applications. Several steps of manual radiosynthesis and post-labeling purification often cause significant radiation exposure to radiopharmacists. Of course, this problem can be solved by developing preparative modules for routine radiosynthesis, which will definitely lead to added cost for the radiotracer. Thus, this is a continuing need for more efficient integrin $\alpha_v\beta_3$-specific radiotracers that are readily prepared from a kit formulation without further post-labeling chromatographic purification.

Maximizing Binding Affinity via Multimerization

Cyclization to Improve Binding Affinity and Selectivity

Many cyclic RGD peptides have been proposed as the integrin $\alpha_v\beta_3$ antagonists for treatment of cancer. It was found that incorporation of the RGD sequence into a cyclic pentapeptide framework (Figure 3) increases the binding affinity and selectivity for integrin $\alpha_v\beta_3$ over glycoprotein IIb/IIIa (110–113). After extensive structure-activity evaluations, it was concluded that the amino acid in position 5 has no significant impact on integrin $\alpha_v\beta_3$ binding affinity. The valine (V) residue in c(RGDfV) can be replaced by lysine (K) or glutamic acid (E) to afford c(RGDfK) and c(RGDfE), respectively, without changing the integrin $\alpha_v\beta_3$ binding affinity.

Cyclic RGD Dimers

To improve integrin $\alpha_v\beta_3$ binding affinity, multimeric RGD peptides, such as E[c(RGDfK)]$_2$, have been used to develop integrin $\alpha_v\beta_3$-targeted radiotracers. For example, Rajopadhye et al were the first to use cyclic RGD dimers, such as E[c(RGDfK)]$_2$ (Figure 4), to develop diagnostic (^{99m}Tc) and therapeutic (^{90}Y and ^{64}Cu) radiotracers (56,57,114,115). Recently, Chen et al (50,51) reported the ^{64}Cu and ^{18}F-labeled E[c(RGDyK)]$_2$ (Figure 4) as PET radiotracers. Poethko et al found that the RGDfE dimer [c(RGDfE)HEG]$_2$-K-Dpr-[^{18}F]FBOA (Figure 4) had much better targeting capability as evidenced by its higher integrin $\alpha_v\beta_3$ binding affinity and tumor uptake as compared to its monomeric analog c(RGDfE)HEG-Dpr-[^{18}F]FBOA (40–42).

Cyclic RGD Tetramers and Octamers

Several groups have used the multimer concept to prepare cyclic RGD tetramers and octamers. For example, Boturyn et al reported a series of cyclic RGDfK tetramers (116), and found that increasing the peptide multiplicity significantly enhanced the integrin $\alpha_v\beta_3$ binding affinity and internalization. Kessler et al reported a cyclic RGDfE tetramer (Figure 5) that had better integrin $\alpha_v\beta_3$ binding affinity than its monomeric and dimeric analogs (40–42). Liu et al reported the use a cyclic RGDfK tetramer E[E[c(RGDfK)]$_2$]$_2$ (Figure 5) for development of integrin $\alpha_v\beta_3$-targeted SPECT and PET radiotracers (52,64–68). Chen et al recently used ^{64}Cu and ^{18}F-labeled cyclic RGD tetramer E[E[c(RGDxK)]$_2$]$_2$ and octamer E[E[E[c(RGDyK)]$_2$]$_2$]$_2$ for tumor imaging by PET (52,117). Although the results from both in vitro assays and ex-vivo biodistribution studies have demonstrated that radiolabeled (^{99m}Tc, ^{18}F and ^{64}Cu) RGD tetramers and octamer have much better tumor targeting capability (higher integrin $\alpha_v\beta_3$ binding affinity and better radiotracer tumor uptake) than their dimeric analogs, it remains unclear if the cyclic RGD motifs in E[E[c(RGDxK)]$_2$]$_2$ (x = f and y) and E[E[E[c(RGDyK)]$_2$]$_2$]$_2$ are really multivalent in binding to integrin $\alpha_v\beta_3$. As the peptide multiplicity increases, the uptake of radiolabeled multimeric RGD peptides in the kidneys, liver, lungs and spleen are also significantly increased. In addition, the cost for E[E[c(RGDfK)]$_2$]$_2$ and E[E[E[c(RGDyK)]$_2$]$_2$]$_2$ is prohibitively high for development of integrin $\alpha_v\beta_3$-targeted radiotracers in the future. Thus, an alternate approach is needed to improve integrin $\alpha_v\beta_3$-targeting capability and minimize the radiotracer accumulation in non-cancerous organs.

Maximizing Binding Affinity via Bivalency

Factors Influencing Binding Affinity

The success of E[c(RGDfK)]$_2$ as targeting biomolecules is very intriguing. Given the short distance (6 bonds excluding side-arms of K-residues) between two cyclic RGD motifs in E[c(RGDfK)]$_2$, it is unlikely that they would bind to two adjacent integrin $\alpha_v\beta_3$ sites simultaneously. However, the binding of one RGD motif to integrin $\alpha_v\beta_3$ will significantly increase the “local concentration” of second RGD motif in the vicinity of integrin $\alpha_v\beta_3$ sites (Figure 6A). The “locally enhanced RGD concentration” may explain the higher tumor uptake of radiolabeled (^{99m}Tc, ^{111}In, ^{90}Y, ^{18}F and ^{64}Cu) cyclic RGD dimers as compared to their monomeric analogs (60–65). To further improve the integrin $\alpha_v\beta_3$-targeting capability of cyclic RGD dimers, the distance between two cyclic RGD motifs must be increased so that they are to achieve simultaneous integrin $\alpha_v\beta_3$ binding (Figure 6B). The combination of “bivalency” and the “enriched local RGD concentration” is expected to result in higher integrin $\alpha_v\beta_3$ targeting capability of cyclic RGD dimers and better tumor uptake with longer tumor retention time for their corresponding radiotracers.

Improve Integrin $\alpha_v\beta_3$ Binding Affinity by Increasing Distance between Cyclic RGD Motifs

To demonstrate this concept, Shi et al recently reported a series of cyclic RGD peptide dimers (Figure 7) containing triglycine (G_3) and PEG_4 linkers, which are used to increase the distance between two cyclic RGD motifs from 6 bonds in $E[c(RGDfK)]_2$ to 24 bonds in $3G_3$-dimer and 38 bonds in $3PEG_4$-dimer (118,119). The integrin $\alpha_v\beta_3$ binding affinities (Table 1) against ^{125}I-echistatin bound to U87MG human glioma cells follow the order of HYNIC-tetramer (IC_{50} = 7 ± 2 nM) > HYNIC-$2PEG_4$-dimer (IC_{50} = 52 ± 7 nM) ~ HYNIC-$3PEG_4$-dimer (IC_{50} = 60 ± 4 nM) ~ HYNIC-$3G_3$-dimer (IC_{50} = 61 ± 2 nM) > HYNIC-PEG_4-dimer (IC_{50} = 84 ± 7 nM) ~ HYNIC-dimer (IC_{50} = 112 ± 21 nM) ≫ HYNIC-G_3-monomer (IC_{50} = 358 ± 8 nM) > HYNIC-PEG_4-monomer (IC_{50} = 452 ± 11 nM). These data indicate that the G_3 and PEG_4 linkers between two RGD motifs are responsible for the improved integrin $\alpha_v\beta_3$ affinity of HYNIC-$3G_3$-dimer and HYNIC-$3PEG_4$-dimer as compared to that of HYNIC-PEG_4-dimer. The higher binding affinity of HYNIC-tetramer is probably due to its two extra cyclic RGD motifs.

It is very important to note that the IC_{50} value depends largely on the radioligand (^{125}I-c(RGDyK) vs. ^{125}I-echistatin) and tumor cell lines (U87MG vs. MDA-MB-435) used in the competitive displacement assay. Caution should be taken when comparing the IC_{50} values of cyclic RGD peptides with those reported in the literature. Whenever possible, a “control compound”, such as c(RGDfK) or c(RGDyK) should be used in each experiment.

Ternary ligand complexes [^{99m}Tc(HYNIC-$3PEG_4$-dimer)(tricine)(TPPTS)] (^{99m}Tc-$3PEG_4$-dimer) and [^{99m}Tc(HYNIC-$3G_3$-dimer)(tricine)(TPPTS)] (^{99m}Tc-$3G_3$-dimer) have been evaluated in the athymic nude mice bearing U87MG glioma and MDA-MB-435 breast tumor xenografts (118,119). For comparison purposes, [^{99m}Tc(HYNIC-PEG_4-dimer)(tricine)(TPPTS)] (^{99m}Tc-PEG_4-dimer) and [^{99m}Tc(HYNIC-tetramer)(tricine)(TPPTS)] (^{99m}Tc-tetramer) were also evaluated in the same tumor-bearing animal model (118,119). As expected, the breast tumor uptake of ^{99m}Tc-$3PEG_4$-dimer and ^{99m}Tc-$3G_3$-dimer was comparable to that of ^{99m}Tc-tetramer (Figure 8A), and was >2x higher than that of ^{99m}Tc-PEG_4-dimer (118). These data suggest that $3PEG_4$-dimer, $3G_3$-dimer and tetramer are most likely “bivalent” (Figure 6B) whereas PEG_4-dimer is monodentate (Figure 6A). If PEG_4-dimer were bivalent, HYNIC-PEG_4-dimer would have shared similar integrin $\alpha_v\beta_3$ binding affinity with HYNIC-$3PEG_4$-dimer and HYNIC-$3G_3$-dimer while ^{99m}Tc-PEG_4-dimer would have had the tumor uptake comparable to that of ^{99m}Tc-$3PEG_4$-dimer and ^{99m}Tc-$3G_3$-dimer. In addition, ^{99m}Tc-$3PEG_4$-dimer and ^{99m}Tc-$3G_3$-dimer had the kidney and liver uptake that was half of that for ^{99m}Tc-tetramer, probably because $3PEG_4$-dimer and $3G_3$-dimer have only two RGD motifs. Therefore, ^{99m}Tc-$3PEG_4$-dimer and ^{99m}Tc-$3G_3$-dimer have significant advantages over ^{99m}Tc-tetramer with respect to T/B ratios (118,119).

Multimeric ≠ Multivalent

It is critical to note that multimeric RGD peptides are not necessarily multivalent. There are two factors (bivalency and enhanced local RGD concentration) contributing to high integrin $\alpha_v\beta_3$ binding affinity of multimeric RGD peptides. The concentration factor exists in all multimeric RGD peptides regardless of the linkers. The key for bivalency is the distance between two cyclic RGD motifs. For example, this distance in $3PEG_4$-dimer (38 bonds) and $3G_3$-dimer (26 bonds) is long enough for them to achieve bivalency, which leads to the higher integrin $\alpha_v\beta_3$ binding affinity of HYNIC-$3PEG_4$-dimer and HYNIC-$3G_3$-dimer than that of HYNIC-PEG_4-dimer, and the much higher breast tumor uptake (Figure 8A) for ^{99m}Tc-$3PEG_4$-dimer and ^{99m}Tc-$3G_3$-dimer as compared to that of ^{99m}Tc-PEG_4-dimer. In contrast, the concentration factor is responsible for the better binding affinity of HYNIC-tetramer than that of HYNIC-$3PEG_4$-dimer and HYNIC-$3G_3$-dimer. The fact that the breast tumor uptake of ^{99m}Tc-$3PEG_4$-dimer and ^{99m}Tc-$3G_3$-dimer is comparable to that of ^{99m}Tc-

tetramer suggests that the contribution from the "concentration factor" might not be as significant as that from the "bivalency factor". In addition, the ability of a multimeric RGD peptide to achieve bivalency also depends on the integrin $\alpha_v\beta_3$ density. If the tumor integrin $\alpha_v\beta_3$ density is high, the distance between two neighboring integrin $\alpha_v\beta_3$ sites will be short, which makes it easier for the multimeric RGD peptide to achieve bivalency. If the integrin $\alpha_v\beta_3$ density is very low, the distance between two neighboring integrin $\alpha_v\beta_3$ sites will be long, and it might be more difficult for the same multimeric RGD peptide to achieve simultaneous integrin $\alpha_v\beta_3$ binding.

Relationship between Tumor Size and Radiotracer Tumor Uptake

The ability to quantify the integrin $\alpha_v\beta_3$ in vivo provides opportunities to select the patients more appropriately for anti-angiogenic treatment and to monitor the therapeutic efficacy of integrin $\alpha_v\beta_3$-positive tumors (120,121). The %ID tumor uptake reflects the total integrin $\alpha_v\beta_3$ level while the %ID/g tumor uptake reflects the integrin $\alpha_v\beta_3$ density. Figure 8B shows the relationship between tumor size and tumor uptake (%ID and %ID/g) of ^{99m}Tc-3PEG$_4$-dimer. There was a linear relationship between tumor size and %ID tumor uptake with R^2 = 0.9164 (Figure 8B), suggesting that ^{99m}Tc-3PEG$_4$-dimer might be useful for monitoring tumor growth during anti-angiogenic therapy (118). If the tumor uptake is expressed as %ID/g (Figure 8C), it seems that ^{99m}Tc-3PEG$_4$-dimer has a narrow window to achieve an optimal tumor uptake. When tumor size is small (<0.05 g), there is little angiogenesis with low blood flow, and ^{99m}Tc-3PEG$_4$-dimer has low %ID/g tumor uptake. When the tumor size is 0.1 g–0.25 g, the microvessel density and integrin $\alpha_v\beta_3$ density are high. The %ID/g tumor uptake of ^{99m}Tc-3PEG$_4$-dimer is ~10 %ID/g (Figure 8C). As tumors grow, the total integrin $\alpha_v\beta_3$ level is higher, and the %ID tumor uptake increases (Figure 8B). However, the microvessel density decreases due to maturity of blood vessels. The integrin $\alpha_v\beta_3$ density also decreases due to larger interstitial space (122). In addition, parts of the tumor may become necrotic, leading to the lower integrin $\alpha_v\beta_3$ density. As a result, larger tumors have lower %ID/g tumor uptake than smaller ones (Figure 8C).

Radiotracer Tumor Uptake and Tumor Cell Integrin $\alpha_v\beta_3$ Expression

Figure 9 compares the tumor uptake of ^{99m}Tc-3PEG$_4$-dimer and ^{99m}Tc-3G$_3$-dimer in athymic nude mice bearing U87MG glioma and HT29 colon cancer xenografts, and the integrin $\alpha_v\beta_3$ expression levels on U87MG glioma and HT29 cells. Both ^{99m}Tc-3PEG$_4$-dimer and ^{99m}Tc-3G$_3$-dimer have significantly higher uptake (%ID/g) in the glioma than HT29 tumors (Figure 9: top), which is supported by the presence of higher level of integrin $\alpha_v\beta_3$ expression on U87MG glioma cells than those on HT29 cells (Figure 9: bottom). These data clearly show that the integrin $\alpha_v\beta_3$ level on tumor cells (U87MG > HT29) plays a significant role in the radiotracer tumor uptake. More fluorescent staining studies are needed to better quantify the contributions from the integrin $\alpha_v\beta_3$ expressed on the tumor cells and neovasculature in the tumor tissue.

^{64}Cu(DOTA-3PEG$_4$-dimer) and ^{64}Cu(DOTA-3G$_3$-dimer)

Recently, Shi et al (123) reported two cyclic RGD dimer conjugates: DOTA-3PEG$_4$-dimer and DOTA-3G$_3$-dimer (Figure 10). It was found that the integrin $\alpha_v\beta_3$ binding affinity (Table 1) follow the order of DOTA-tetramer (IC_{50} = 10 ± 2 nM) > DOTA-3G$_3$-dimer (IC_{50} = 74 ± 3 nM) ~ DOTA-3PEG$_4$-dimer (IC_{50} = 62 ± 6, nM) > DOTA-dimer (IC_{50} = 102 ± 5 nM) against ^{125}I-echistatin bound to U87MG glioma cells. Once again, bivalency is likely responsible for the higher integrin $\alpha_v\beta_3$ binding affinity of DOTA-3PEG$_4$-dimer and DOTA-3G$_3$-dimer than that of DOTA-dimer. This conclusion is completely consistent with the higher tumor uptake of ^{64}Cu(DOTA-3PEG$_4$-dimer) and ^{64}Cu(DOTA-3G$_3$-dimer) than that of ^{64}Cu(DOTA-dimer) (123). In contrast, the concentration factor is most likely responsible

for higher integrin $\alpha_v\beta_3$ binding affinity of DOTA-tetramer than that of DOTA-3PEG$_4$-dimer and DOTA-3G$_3$-dimer, and the higher initial tumor uptake of ^{64}Cu(DOTA-tetramer) as compared to that of ^{64}Cu(DOTA-3PEG$_4$-dimer) and ^{64}Cu(DOTA-3G$_3$-dimer) (132). However, the uptake of ^{64}Cu(DOTA-3PEG$_4$-dimer) in the liver and kidneys was significantly lower than that reported for ^{64}Cu(DOTA-tetramer) (57), due to the presence of four R-residues in E[E[c(RGDfK)]$_2$]$_2$ as compared to only two R-residues in ^{64}Cu(DOTA-3PEG$_4$-dimer) and ^{64}Cu(DOTA-3G$_3$-dimer) (132).

^{111}In(DOTA-3PEG$_4$-dimer) and ^{111}In(DOTA-3G$_3$-dimer)

To explore the impact of radiometal chelates, ^{111}In(DOTA-3PEG$_4$-dimer) and ^{111}In (DOTA-3G$_3$-dimer) were evaluated in the same animal model (124). ^{111}In(DOTA-3PEG$_4$-dimer) and ^{111}In(DOTA-3G$_3$-dimer) share the same DOTA chelator, have almost identical lipophilicity (log P = −4.13 ± 0.08 and −4.20 ± 0.21, respectively), and show very similar metabolic stability (124). The tumor uptake of ^{111}In(DOTA-3G$_3$-dimer) is comparable to that of ^{111}In(DOTA-3PEG$_4$-dimer) (Figure 11A). Planar imaging studies showed that they both had very high tumor uptake with a long tumor retention and excellent tumor-to-background contrast (124). The activity accumulation in the chest and abdominal regions almost completely disappeared at 60 min p.i. The combination of the hydrophilic ^{111}In(DOTA) chelate with PEG$_4$/G$_3$ linkers is responsible for the low liver uptake for ^{111}In(DOTA-3PEG$_4$-dimer) and ^{111}In(DOTA-3G$_3$-dimer), leading to high tumor/liver ratios (Figure 11A). Both ^{111}In (DOTA-3PEG$_4$-dimer) and ^{111}In(DOTA-3G$_3$-dimer) also had low kidney and muscle uptake with very high tumor/kidney and tumor/muscle ratios (124). Their integrin $\alpha_v\beta_3$-specificity has been clearly demonstrated by the blocking experiment, in which ^{111}In(DOTA-3PEG$_4$-dimer) was used as the radiotracer and E[c(RGDfK)]$_2$ as the blocking agent (124). The RGD-specificity of ^{111}In-labeled cyclic RGD dimers was demonstrated by the higher integrin $\alpha_v\beta_3$ affinity of DOTA-3PEG$_4$-NS (IC_{50} = 715 ± 45 nM; 3PEG$_4$-NS = PEG$_4$-E[PEG$_4$-(RGKfD)]$_2$, a scrambled nonsense peptide) than that of DOTA-3PEG$_4$-dimer (1.3 ± 0.3 nM), and the much better tumor uptake of ^{111}In(DOTA-3PEG$_4$-dimer) (10.06 ± 3.52 %ID/g) than that of ^{111}In(DOTA-3PEG$_4$-NS) (0.30 ± 0.09 %ID/g) in the same animal model. On the basis of the integrin $\alpha_v\beta_3$- and RGD-specificity of the ^{111}In-labeled cyclic RGD peptides, it has been suggested that their uptake in several normal organs (e.g. intestine, kidneys, liver, lungs and spleen) might be also integrin $\alpha_v\beta_3$-mediated (124).

^{111}In(DOTA-3PEG$_4$-dimer) and ^{64}Cu(DOTA-3PEG$_4$-dimer) share the same DOTA-conjugate. In spite of their difference in radiometal, the tumor uptake ^{111}In(DOTA-3PEG$_4$-dimer) (10.89 ± 2.55 and 7.65 ± 3.17 %ID/g at 30and 240 min p.i., respectively) was close to that of ^{64}Cu(DOTA-3PEG$_4$-dimer) (8.23 ± 1.97 and 6.43 ± 1.22 %ID/g at 30 and 240 min p.i., respectively). They also share similar uptake in normal organs. For example, the kidney uptake of ^{111}In(DOTA-3PEG$_4$-dimer) was 5.80 ± 0.95 and 2.78 ± 0.20 %ID/g at 30 and 240 min p.i., respectively, and was comparable to that of ^{64}Cu(DOTA-3PEG$_4$-dimer) (6.59 ± 0.93 %ID/g at 30 min p.i. and 2.81 ± 0.36 % ID/g at 240 min p.i.). The liver uptake of ^{111}In (DOTA-3PEG$_4$-dimer) is 2.52 ± 0.57 %ID/g at 30 min and 1.61 ± 0.06 %ID/g at 240 min p.i. while ^{64}Cu(DOTA-3PEG$_4$-dimer) has the liver uptake of 2.80 ± 0.35 %ID/g at 30 min p.i. and 1.87 ± 0.51 %ID/g at 240 min p.i. Similar conclusion can be made by comparing biodistribution properties of ^{64}Cu(DOTA-3G$_3$-dimer) and ^{111}In(DOTA-3G$_3$-dimer). These data suggest that the radiometal chelate (Figure 11B) has minimal impact on radiotracer tumor uptake and excretion kinetics.

^{68}Ga(NOTA-2PEG$_4$-dimer) and ^{68}Ga(NOTA-2G$_3$-dimer)

We also prepared conjugates NOTA-2PEG$_4$-dimer and NOTA-2G$_3$-dimer (Figure 12: NOTA = 1,4,7-triaazacyclononane-1,4,7-tetracetic acid) and their ^{68}Ga complexes, ^{68}Ga (NOTA-2PEG$_4$-dimer) and ^{68}Ga(NOTA-2G$_3$-dimer) (125). The integrin $\alpha_v\beta_3$ binding affinity

(Table 1) of NOTA-dimer (IC_{50} = 100 ± 3 nM), NOTA-2G_3-dimer (IC_{50} = 66 ± 4 nM) and NOTA-2PEG_4-dimer (IC_{50} = 54 ± 2 nM) were very close to those for DOTA-dimer (IC_{50} = 102 ± 5 nM), DOTA-3G_3-dimer (IC_{50} = 74 ± 3 nM) and DOTA-3PEG_4-dimer (IC_{50} = 62 ± 6 nM), respectively. These data further suggest that the G_3 and PEG_4 linkers between cyclic RGD motifs in dimeric RGD peptides make it possible for them to bind integrin $\alpha_v\beta_3$ in a bivalent fashion. The tumor uptake of ^{68}Ga(NOTA-2G_3-dimer) and ^{68}Ga(NOTA-2PEG_4-dimer) was much higher than that of ^{68}Ga(NOTA-dimer) in the same tumor-bearing animal model (125), suggesting that the addition of G_3 and PEG_4 linkers between two cyclic RGD motifs increases the radiotracer tumor uptake. In all cases, the tumors can be clearly visualized as early as 30 min p.i. with excellent contrast (Figure 12). It was also found that the tumor uptake of ^{68}Ga(NOTA-2PEG_4-dimer) in MDA-MB-435 breast tumor was significantly lower than that in U87MG glioma. Similar results were also obtained for ^{18}F-labeled 3PEG_4-dimer (126), which is consistent with that fact that the MDA-MB-435 breast tumors have lower integrin $\alpha_v\beta_3$ expression than U87MG glioma (52–55).

Conclusions

Over the last several years, many multimeric cyclic RGD peptides have been used to increase the integrin $\alpha_v\beta_3$–targeting capability. It was found that increasing the peptide multiplicity can significantly enhance their integrin $\alpha_v\beta_3$ binding affinity, and improve the radiotracers tumor targeting ability. However, as peptide multiplicity increases, the uptake of radiolabeled multimeric RGD peptides is also significantly increased in normal organs. There is no significant advantage in using radiolabeled tetramers $E\{E[c(RGDxK)]_2\}_2$ (x = f and y) over their dimeric analogs $E[c(RGDxK)]_2$ (x = f and y) with respect to T/B ratios. In addition, the cost for $E\{E[c(RGDxK)]_2\}_2$ (x = f and y), $E\{E[E[c(RGDyK)]_2]_2\}_2$ is too high for them to be useful for future radiotracer development.

Recent studies on cyclic RGD dimers suggest that two factors (bivalency and enhanced local RGD concentration) contribute to the high integrin $\alpha_v\beta_3$ binding affinity of multimeric cyclic RGD peptides (118,119,123–126). The concentration factor exists in all multimeric RGD peptides regardless of the linker length between two cyclic RGD motifs. To achieve bivalency, the distance between two RGD motifs must be long enough for them to bind the neighboring integrin $\alpha_v\beta_3$ sites simultaneously. Among the cyclic RGD peptides, 2PEG_4-dimer/3PEG_4-dimer and 2G_3-dimer/3G_3-dimer show most promising results with respect to the tumor uptake and T/B ratios of their radiotracers (^{99m}Tc, ^{111}In, ^{64}Cu and ^{68}Ga). Thus, 2PEG_4-dimer/3PEG_4-dimer and 2G_3-dimer/3G_3-dimer are better integrin $\alpha_v\beta_3$-targeting biomolecules than the tetramer $E\{E[c(RGDfK)]_2\}_2$ with respect to their cost and the T/B ratios of their ^{99m}Tc, ^{111}In, ^{64}Cu and ^{68}Ga radiotracers.

While current research efforts on the integrin $\alpha_v\beta_3$–targeted radiotracers have been focused on new cyclic RGD peptides, the formulation development for routine preparation of radiotracers is often neglected. It must be emphasized that it is common to use post-labeling chromatographic separation for improvement of radiotracer purity and specific activity for research purposes. In clinical settings, however, post-labeling purification is not practical. Regardless of the beauty of the science involved in the discovery of a new radiotracer, its success relies largely on the availability and capability to improve the quality of cancer patient's life. As a matter of fact, the main challenge for [^{18}F]Galacto-RGD and [^{18}F]-AH111585 to assume a wide-spread clinical utility is not their biological performance, but their clinical availability at reasonable cost. In this respect, the integrin $\alpha_v\beta_3$-targeted ^{99m}Tc radiotracers will offer significant advantages over their corresponding ^{18}F analogs because of the clinical availability of ^{99}Mo-^{99m}Tc generators, and the kit formulation for routine preparation of ^{99m}Tc radiotracers at low cost. However, both planar imaging and SPECT suffer a significant

drawback with respect to quantification of the radiotracer "absolute" organ uptake, the speed of dynamic imaging, spatial resolution and tissue attenuation.

The successful application of the ^{68}Ga-labeled somatostatin analogs for imaging tumors in cancer patients has clearly demonstrated that ^{68}Ga is an excellent alternative to ^{18}F. ^{68}Ga is available from an in-house commercially available ^{68}Ge/^{68}Ga generator (127–129), and its short half-life is best suited for the fast excretion kinetics of many ^{68}Ga-labeled small peptides. ^{64}Cu is another viable alternative to ^{18}F. The use of NOTA and its derivatives as BFCs allows the development of the kit formulation for routine preparation of ^{68}Ga and ^{64}Cu radiotracers with high specific activity. In addition, ^{68}Ga(NOTA) and ^{64}Cu(NOTA) chelates have very high hydrophilicity, which is extremely important for improving the radiotracer clearance kinetics from non-cancerous organs.

It is very important to note that integrin $\alpha_v\beta_3$ is also overexpressed on the activated endothelial cells during wound healing and post-infarct remodeling, in rheumatoid arthritis, and atherosclerotic plaque (1–4,130,131). The integrin $\alpha_v\beta_3$–targeted radiotracers have been proposed for imaging myocardial angiogenesis (132), inflammatory diseases (133), and hindlimb ischemia (134). Recent results showed that the ^{111}In-labeled nonpeptide integrin $\alpha_v\beta_3$ antagonist (RP748) was able to image the angiogenesis in the heart with myocardial infarction (132), and the radiotracer uptake in the infarct region was associated with the integrin $\alpha_v\beta_3$ expression level. The results reported by Pichler et al suggest that [^{18}F]Galacto-RGD might be a powerful tool to distinguish between acute and chronic phases of T-cell mediated immune responses (133). Studies have also demonstrated the value of a ^{99m}Tc-labeled cyclic RGD monomer (NC100692) for imaging the integrin $\alpha_v\beta_3$ in rodent models of hindlimb ischemia (134). These promising results suggest that the newer and more effective integrin $\alpha_v\beta_3$–targeted radiotracers under development for tumor imaging might become valuable non-invasive markers of angiogenesis after ischemic injury, myocardial infarction and inflammation. In addition, the combination of high tumor uptake, long tumor retention with favorable pharmacokinetic of ^{111}In(DOTA-3G$_3$-dimer) and ^{111}In(DOTA-3PEG$_4$-dimer) suggests that their corresponding ^{90}Y and ^{177}Lu analogs, M(DOTA-RGD) (M = ^{90}Y and ^{177}Lu; and RGD = 3G$_3$-dimer and 3PEG$_4$-dimer), might be useful for the treatment of integrin $\alpha_v\beta_3$-positive tumors.

Acknowledgments

The author would like to thank Dr. Xiaoyuan Chen at Stanford Medical School and Dr. Fan Wang at the Beijing University Medical Isotopes Research Center for their collaboration on the radiolabeled multimeric cyclic RGD peptides. This work is supported, in part, by Purdue University and research grants: R01 CA115883 A2 (S.L.) from the National Cancer Institute (NCI) and DE-FG02-08ER64684 from the Department of Energy.

References

1. Folkman J. Angiogenesis in cancer, vascular, rheumatoid and other disease. Nat Med 1995:27–31. [PubMed: 7584949]
2. Mousa SA. Mechanism of angiogenesis in vascular disorders: potential therapeutic targets. Drugs of the Future 1998;23:51–60.
3. Carmeliet P. Mechanisms of angiogenesis and arteriogenesis. Nat Med 2000;6:389–395. [PubMed: 10742145]
4. Meitar D, Crawford SE, Rademaker AW, Cohn SL. Tumor angiogenesis correlates with metastatic disease, N-*myc*-amplification, and poor outcome in human neuroblastoma. J Clin Oncol 1996;14:405–414. [PubMed: 8636750]
5. Gasparini G, Brooks PC, Biganzoli E, Vermeulen PB, Bonoldi E, Dirix LY, Ranieri G, Miceli R, Cheresh DA. Vascular integrin $\alpha_v\beta_3$: a new prognostic indicator in breast cancer. Clin Can Res 1998;4:2625–2634.

6. Falcioni R, Cimino L, Gentileschi MP, D'Agnano I, Zupi G, Kennel SJ, Sacchi A. Expression of beta 1, beta 3, beta 4, and beta 5 integrins by human lung carcinoma cells of different histotypes. Exp Cell Res 1994;210:113–122. [PubMed: 7505746]
7. Sengupta S, Chattopadhyay N, Mitra A, Ray S, Dasgupta S, Chatterjee A. Role of $\alpha_v\beta_3$ integrin receptors in breast tumor. J Exp Clin Cancer Res 2001;20:585–590. [PubMed: 11876555]
8. Bögler O, Mikkelsen T. Angiogenesis in Glioma: molecular mechanisms and roadblocks to translation. Cancer J 2003;9:205–213. [PubMed: 12952305]
9. Folkman J. Role of angiogenesis in tumor growth and metastasis. Semin Oncol 2002;29:15–18. [PubMed: 12516034]
10. Hwang R, Varner JV. The role of integrins in tumor angiogenesis. Hematol Oncol Clin North Am 2004;18:991–1006. [PubMed: 15474331]
11. Brooks PC, Clark RAF, Cheresh DA. Requirement of vascular integrin $\alpha_v\beta_3$ for angiogenesis. Science 1994;264:569–571. [PubMed: 7512751]
12. Friedlander M, Brooks PC, Shaffer RW, Kincaid CM, Varner JA, Cheresh DA. Definition of two angiogenic pathways by distinct α_v integrin. Science 1995;270:1500–1502. [PubMed: 7491498]
13. Horton MA. The $\alpha_v\beta_3$ integrin "vitronectin receptor". Int J Biochem Cell Biol 1997;29:721–725. [PubMed: 9251239]
14. Bello L, Francolini M, Marthyn P, Zhang JP, Carroll RS, Nikas DC, Strasser JF, Villani R, Cheresh DA, Black PM. Alpha(v)beta3 and alpha(v)beta5 integrin expression in glioma periphery. Neurosurgery 2001;49:380–389. [PubMed: 11504114]
15. Albelda SM, Mette SA, Elder DE, Stewart RM, Damjanovich L, Herlyn M, Buck CA. Integrin distribution in maliganant melanoma: association of the beta3 subunit with tumor progression. Cancer Res 1990;50:6757–6764. [PubMed: 2208139]
16. Felding-Habermann B, Mueller BM, Romerdahl CA, Cheresh DA. Involvement of integrin alpha V gene expression in human melanoma tumorigenicity. J Clin Invest 1992;89:2018–2022. [PubMed: 1376331]
17. Zitzmann S, Ehemann V, Schwab M. Arginine-Glycine-Aspartic acid (RGD)-peptide binds to both tumor and tumor endothelial cells in vivo. Cancer Res 2002;62:5139–5143. [PubMed: 12234975]
18. Weber WA, Haubner R, Vabuliene E, Kuhnast B, Webster HJ, Schwaiger M. Tumor angiogenesis targeting using imaging agents. Q J Nucl Med 2001;45:179–182. [PubMed: 11476168]
19. Costouros NG, Diehn FE, Libutti SK. Molecular imaging of tumor angiogenesis. J Cell Biol Suppl 2002;39:72–78.
20. van de Wiele C, Oltenfreiter R, De Winter O, Signore A, Slegers G, Dierckx RA. Tumor angiogenesis pathways: related clinical issues and implications for nuclear medicine imaging. Eur J Nucl Med 2002;29:699–709.
21. Liu S, Edwards DS. Fundamentals of receptor-based diagnostic metalloradiopharmaceuticals. Topics in Current Chem 2002;222:259–278.
22. Liu S, Robinson SP, Edwards DS. Integrin $\alpha_v\beta_3$ directed radiopharmaceuticals for tumor imaging. Drugs of the Future 2003;28:551–564.
23. Haubner R, Wester HJ. Radiolabeled tracers for imaging of tumor angiogenesis and evaluation of antiangiogenic therapies. Current Pharmaceutical Design 2004;10:1439–1455. [PubMed: 15134568]
24. D'Andrea LD, Del Gatto A, Pedone C, Benedetti E. Peptide-based molecules in angiogenesis. Chem Biol Drug Des 2006;67:115–126. [PubMed: 16492159]
25. Chen X. Multimodality imaging of tumor integrin $\alpha_v\beta_3$ expression. Mini-Rev Med Chem 2006;6:227–234. [PubMed: 16472190]
26. Liu S. Radiolabeled multimeric cyclic RGD peptides as integrin $\alpha_v\beta_3$-targeted radiotracers for tumor imaging. Mol Pharm 2006;3:472–487. [PubMed: 17009846]
27. Cai W, Chen X. Multimodality Molecular imaging of tumor angiogenesis. J Nucl Med 2008;49:113S–128S. [PubMed: 18523069]
28. Cai W, Niu G, Chen X. Imaging of integrins as biomarkers for tumor angiogenesis. Current Pharmaceutical Design 2008;14:2943–2973. [PubMed: 18991712]
29. Chen X. Advances in anatomic, functional, and molecular imaging of angiogenesis. J Nucl Med 2008;49:511–514. [PubMed: 18375921]

30. Jin H, Varner J. Integrins: roles in cancer development and as treatment targets. Br J Cancer 2004;90:561–565. [PubMed: 14760364]
31. Kumar CC. Integrin $\alpha_v\beta_3$ as a therapeutic target for blocking tumor-induced angiogenesis. Curr Drug Targets 2003;4:123–131. [PubMed: 12558065]
32. Meyer A, Aurenheimer J, Modlinger A, Kessler H. Targeting RGD recognizing integrins: drug development, biomaterial research, tumor imaging and targeting. Current Pharmaceutical Design 2006;12:2723–2747. [PubMed: 16918408]
33. Van Hagen PM, Breeman WAP, Bernard HF, Schaar M, Mooij CM, Srinivasan A, Schmidt MA, Krenning EP, de Jong M. Evaluation of a radiolabeled cyclic DTPA-RGD analog for tumor imaging and radionuclide therapy. Int J Cancer (Radiat Oncol Invest) 2000;90:186–198.
34. Huabner R, Wester HJ, Senekowitsch-Schmidtke R, Diefenbach B, Kessler H, Stöcklin G, Schwaiger M. RGD-peptides for tumor targeting: biological evaluation of radioiodinated analogs and introduction of a novel glycosylated peptide with improved biokinetics. J Labelled Compounds & Radiopharmaceuticals 1997;40:383–385.
35. Sivolapenko GB, Skarlos D, Pectasides D, Stathopoulou E, Milonakis A, Sirmalis G, Stuttle A, Courtenay-Luck NS, Konstantinides K, Epenetos AA. Imaging of metastatic melanoma utilizing a technetium-99m labeled RGD-containing synthetic peptide. Eur J Nucl Med 1998;25:1383–1389. [PubMed: 9818277]
36. Haubner R, Wester HJ, Weber WA, Mang C, Ziegler SI, Goodman SL, Senekowitsch-Schmidtke R, Kessler H, Schwaiger M. Noninvasive imaging of $\alpha_v\beta_3$ integrin expression using ^{18}F-labeled RGD-containing glycopeptide and positron emission tomography. Cancer Res 2001;61:1781–1785. [PubMed: 11280722]
37. Haubner R, Wester HJ, Reuning U, Senekowitsch-Schmidtke R, Diefenbach B, Kessler H, Stöcklin G, Schwaiger M. Radiolabeled $\alpha_v\beta_3$ integrin antagonists: a new class of tracers for tumor imaging. J Nucl Med 1999;40:1061–1071. [PubMed: 10452325]
38. Haubner R, Wester HJ, Burkhart F, Senekowisch-Schmidtke R, Weber W, Goodman SL, Kessler H, Schwaiger M. Glycolated RGD-containing peptides: tracer for tumor targeting and angiogenesis imaging with improved biokinetics. J Nucl Med 2001;42:326–336. [PubMed: 11216533]
39. Haubner R, Bruchertseifer F, Bock M, Kessler H, Schwaiger M, Wester HJ. Synthesis and biological evaluation of ^{99m}Tc-labeled cyclic RGD peptide for imaging the $\alpha_v\beta_3$ expression. Nuklearmedizin 2004;43:26–32. [PubMed: 14978538]
40. Thumshirn G, Hersel U, Goodman SL, Kessler H. Multimeric cyclic RGD peptides as potential tools for tumor targeting: solid-phase peptide synthesis and chemoselective oxime ligation. Chem Eur J 2003;9:2717–2725.
41. Poethko T, Schottelius M, Thumshirn G, Herz M, Haubner R, Henriksen G, Kessler H, Schwaiger M, Wester HJ. Chemoselective pre-conjugate radiohalogenation of unprotected mono- and multimeric peptides via oxime formation. Radiochim Acta 2004;92:317–327.
42. Poethko T, Schottelius M, Thumshirn G, Hersel U, Herz M, Henriksen G, Kessler H, Schwaiger M, Wester HJ. Two-step methodology for high yield routine radiohalogenation of peptides: ^{18}F-labeled RGD and octreotide analogs. J Nucl Med 2004;5:892–902. [PubMed: 15136641]
43. Alves S, Correia JDG, Gano L, Rold TL, Prasanphanich A, Haubner R, Rupprich M, Alberto R, Decristoforo C, Santos I, Smith CJ. In vitro and in vivo evaluation of a novel ^{99m}Tc(CO)$_3$-pyrazolyl conjugate of *cyclo*-(Arg-Gly-Asp-D-Tyr-Lys). Bioconj Chem 2007;8:530–537.
44. Fani M, Psimadas D, Zikos C, Xanthopoulos S, Loudos GK, Bouziotis P, Varvarigou AD. Comparative evaluation of linear and cyclic ^{99m}Tc-RGD peptides for targeting of integrins in tumor angiogenesis. Anticancer Res 2006;26:431–434. [PubMed: 16475729]
45. Su ZF, Liu G, Gupta S, Zhu Z, Rusckowski M, Hnatowich DJ. In vitro and in vivo evaluation of a technetium-99m-labeled cyclic RGD peptide as specific marker of $\alpha_v\beta_3$ integrin for tumor imaging. Bioconj Chem 2002;13:561–570.
46. Decristoforo C, Faintuch-Linkowski B, Rey A, von Guggenberg E, Rupprich M, Hernandez-Gonzales I, Rodrigo T, Haubner R. [^{99m}Tc]HYNIC-RGD for imaging integrin $\alpha_v\beta_3$ expression. Nucl Med Biol 2006;33:945–952. [PubMed: 17127166]

47. Chen X, Park R, Tohme M, Shahinian AH, Bading JR, Conti PS. MicroPET and autoradiographic imaging of breast cancer α_v-integrin expression using ^{18}F- and ^{64}Cu-labeled RGD peptide. Bioconj Chem 2004;15:41–49.
48. Chen X, Park R, Shahinian AH, Tohme M, Khankaldyyan V, Bozorgzadeh MH, Bading JR, Moats R, Laug WE, Conti PS. ^{18}F-labeled RGD peptide: initial evaluation for imaging brain tumor angiogenesis. Nucl Med Biol 2004;31:179–189. [PubMed: 15013483]
49. Chen X, Park R, Shahinian AH, Bading JR, Conti PS. Pharmacokinetics and tumor retention of ^{125}I-labeled RGD peptide are improved by PEGylation. Nucl Med Biol 2004;31:11–19. [PubMed: 14741566]
50. Chen X, Liu S, Hou Y, Tohme M, Park R, Bading JR, Conti PS. MicroPET imaging of breast cancer α_v-integrin expression with ^{64}Cu-labeled dimeric RGD peptides. Mol Imag Biol 2004;6:350–359.
51. Chen X, Tohme M, Park R, Hou Y, Bading JR, Conti PS. MicroPET imaging of breast cancer α_v-integrin expression with ^{18}F-labeled dimeric RGD peptide. Mol Imaging 2004;3:96–104. [PubMed: 15296674]
52. Wu Y, Zhang X, Xiong Z, Cheng Z, Fisher DR, Liu S, Gambhir SS, Chen X. MicroPET imaging of glioma integrin $\alpha_v\beta_3$ expression using ^{64}Cu-labeled tetrameric RGD peptide. J Nucl Med 2005;46:1707–1718. [PubMed: 16204722]
53. Zhang X, Xiong Z, Wu Y, Cai W, Tseng JR, Gambhir SS, Chen X. Quantitative PET imaging of tumor integrin $\alpha_v\beta_3$ expression with ^{18}F-FRGD2. J Nucl Med 2006;47:113–121. [PubMed: 16391195]
54. Wu Z, Li Z, Chen K, Cai W, He L, Chin FT, Li F, Chen X. MicroPET of tumor integrin $\alpha_v\beta_3$ expression using ^{18}F-labeled PEGylated tetrameric RGD peptide (^{18}F-FPRGD4). J Nucl Med 2007;48:1536–1544. [PubMed: 17704249]
55. Li ZB, Chen K, Chen X. ^{68}Ga-labeled multimeric RGD peptides for microPET imaging of integrin αvβ3 expression. Eur J Nucl Med Mol Imaging 2008;35:1100–1108. [PubMed: 18204838]
56. Liu S, Cheung E, Rajopadhye M, Ziegler MC, Edwards DS. ^{90}Y- and ^{177}Lu-labeling of a DOTA-conjugated vitronectin receptor antagonist for tumor therapy. Bioconj Chem 2001;12:559–568.
57. Janssen M, Oyen WJG, Massuger LFAG, Frielink C, Dijkgraaf I, Edwards DS, Rajopadhye M, Corsten FHM, Boerman OC. Comparison of a monomeric and dimeric radiolabeled RGD-peptide for tumor targeting. Cancer Biother Radiopharm 2002;17:641–646. [PubMed: 12537667]
58. Janssen M, Oyen WJG, Dijkgraaf I, Massuger LFAG, Frielink C, Edwards DS, Rajopadyhe M, Boonstra H, Corsten FHM, Boerman OC. Tumor targeting with radiolabeled $\alpha_v\beta_3$ integrin binding peptides in a nude mice model. Cancer Res 2002;62:6146–6151. [PubMed: 12414640]
59. Janssen ML, Frielink C, Dijkgraaf I, Oyen WJ, Edwards DS, Liu S, Rajopadhye M, Massuger LF, Corstens FHM, Boerman OC. Improved tumor targeting of radiolabeled RGD-peptides using rapid dose fractionation. Cancer Biother Radiopharm 2004;19:399–404. [PubMed: 15453954]
60. Liu S, Hsieh WY, Kim YS, Mohammed SI. Effect of coligands on biodistribution characteristics of ternary ligand ^{99m}Tc complexes of a HYNIC-conjugated cyclic RGDfK dimer. Bioconj Chem 2005;16:1580–1588.
61. Jia B, Shi J, Yang Z, Xu B, Liu Z, Zhao H, Liu S, Wang F. ^{99m}Tc-labeled cyclic RGDfK dimer: initial evaluation for SPECT imaging of glioma integrin $\alpha_v\beta_3$ expression. Bioconj Chem 2006;17:1069–1076.
62. Liu S, He ZJ, Hsieh WY, Kim YS, Jiang Y. Impact of PKM linkers on biodistribution characteristics of the ^{99m}Tc-labeled cyclic RGDfK dimer. Bioconj Chem 2006;17:1499–1507.
63. Liu S, Hsieh WY, Jiang Y, Kim YS, Sreerama SG, Chen X, Jia B, Wang F. Evaluation of a ^{99m}Tc-labeled cyclic RGD tetramer for noninvasive imaging integrin $\alpha_v\beta_3$-positive breast cancer. Bioconj Chem 2007;18:438–446.
64. Dijkgraaf I, Liu S, Kruijtzer JAW, Soede AC, Oyen WJG, Liskamp RMJ, Corstens FHM, Boerman OC. Effect of linker variation on the in vitro and in vivo characteristics of an ^{111}In-labeled RGD Peptide. Nucl Med Biol 2007;34:29–35. [PubMed: 17210459]
65. Dijkgraaf I, Kruijtzer JAW, Liu S, Soede A, Oyen WJG, Corstens FHM, Liskamp RMJ, Boerman OC. Improved targeting of the $\alpha_v\beta_3$ integrin by multimerization of RGD peptides. Eur J Nucl Med Mol Imaging 2007;34:267–273. [PubMed: 16909226]

66. Liu S, Kim YS, Hsieh WY, Sreerama SG. Coligand effects on solution stability, biodistribution and metabolism of ^{99m}Tc-labeled cyclic RGDfK tetramer. Nucl Med Biol 2008;35:111–121. [PubMed: 18158950]

67. Jia B, Liu Z, Shi J, Yu ZL, Yang Z, Zhao HY, He ZJ, Liu S, Wang F. Linker effects on biological properties of ^{111}In-labeled DTPA conjugates of a cyclic RGDfK dimer. Bioconj Chem 2008;19:201–210.

68. Wang JJ, Kim YS, He ZJ, Liu S. ^{99m}Tc-labeling of HYNIC-conjugated cyclic RGDfK dimer and tetramer using EDDA as coligand. Bioconj Chem 2008;19:634–642.

69. Liu S, Edwards DS. ^{99m}Tc-labeled small peptides as diagnostic radiopharmaceuticals. Chem Rev 1999;99:2235–2268. [PubMed: 11749481]

70. Liu S. The role of coordination chemistry in development of target-specific radiopharmaceuticals. Chem Soc Rev 2004;33:1–18. [PubMed: 14737504]

71. Liu S, Edwards DS. Bifunctional chelators for therapeutic lanthanide radiopharmaceuticals. Bioconj Chem 2001;12:7–34.

72. Jurisson SS, Lydon JD. Potential technetium small molecule radiopharmaceuticals. Chem Rev 1999;99:2205–2218. [PubMed: 11749479]

73. Cai W, Zhang X, Wu Y, Chen X. A thiol-reactive ^{18}F-labeling agent, N-[2-(4-^{18}F-fluorobenzamido) ethyl]maleimide, and synthesis of RGD peptide-based tracer for PET imaging of αvβ3 integrin expression. J Nucl Med 2006;47:1172–1180. [PubMed: 16818952]

74. Welch MJ, McCarthy TJ. The potential role of generator-produced radiopharmaceuticals in clinical PET. J Nucl Med 2000;41:315–317. [PubMed: 10688117]

75. Anderson, CJ.; Green, MA.; Yashi, YF. Chemistry of copper radionuclides and radiopharmaceutical products. In: Welch, MJ.; Redvanly, CS., editors. Handbook of Radiopharmaceuticals: Radiochemistry and Applications. John Wiley & Sons; New York: 2003. p. 402-422.

76. Bormans G, Janssen A, Adriaens P, Crombez D, Witsenboer A, Degoeij J, Mortelmans L, Verbruggen A. ^{62}Zn/^{62}Cu generator for the routine production of ^{62}Cu-PTSM. Appl Radiat Isot 1992;43:1437–1441.

77. Haynes NG, Lacy JL, Nayak N, Martin CS, Dai D, Mathias CJ, Green MA. Performance of a ^{62}Zn/^{62}Cu generator in clinical trials of PET perfusion agent ^{62}Cu-PTSM. J Nucl Med 2000;41:309–314. [PubMed: 10688116]

78. Smith SV. Molecular imaging with copper-64. J Inorg Biochem 2004;98:1874–1901. [PubMed: 15522415]

79. Blower PJ, Lewis JS, Zweit J. Copper radionuclides and radiopharmaceuticals in nuclear medicine. Nucl Med Biol 1996;23:957–980. [PubMed: 9004284]

80. Reichert DE, Lewis JS, Anderson CJ. Metal complexes as diagnostic tools. Coord Chem Rev 1999;184:3–66.

81. Maecke H, Hofmann M, Haberkorn U. ^{68}Ga-labeled peptides in tumor imaging. J Nucl Med 2005;46:172S–178S. [PubMed: 15653666]

82. Heppeler A, Froidevaux S, Eberle AN, Maecke HR. Receptor targeting for tumor localisation and therapy with radiopeptides. Curr Med Chem 2000;7:971–994. [PubMed: 10911025]

83. Heppeler A, Froidevaux S, Mäcke HR, Jermann E, Béhé M, Powell P, Hennig M. Radiometal-labelled macrocyclic chelator-derivatised somatostatin analogue with superb tumour targeting properties and potential for receptor-mediated internal radiotherapy. Chem Eur J 1999;5:1974–1981.

84. Henze M, Schuhmacher J, Hipp P, Kowalski J, Becker DW, Doll F, Mäcke HR, Hofmann M, Debus J, Haberkorn U. PET imaging of somatostatin receptors using [^{68}GA]DOTAD- Phe^{1}-Tyr^{3}-octreotide: first results in patients with meningiomas. J Nucl Med 2001;42:1053–1056. [PubMed: 11438627]

85. Froidevaux S, Eberle AN, Christe M, Sumanovski L, Heppeler A, Schmitt JS, Eisenwiener K, Beglinger C, Mäcke HR. Neuroendocrine tumor targeting: study of novel galliumlabeled somatostatin radiopeptides in a rat pancreatic tumor model. Int J Cancer 2002;98:930–937. [PubMed: 11948475]

86. Hofmann M, Maecke H, Borner AR, Weckesser E, Schoffski P, Oei ML, Schumacher J, Henze M, Heppeler A, Meyer GJ, Knapp WH. Biokinetics and imaging with the somatostatin receptor PET

radioligand ^{68}Ga-DOTATOC: preliminary data. Eur J Nucl Med 2001;28:1751–1757. [PubMed: 11734911]

87. Kowalski J, Henze M, Schuhmacher J, Macke HR, Hofmann M, Haberkorn U. Evaluation of positron emission tomography imaging using ^{68}Ga-DOTA-D Phe(1)-Tyr(^{3})-octreotide in comparison to ^{111}In-DTPAOC SPECT. First results in patients with neuroendocrine tumors. Mol Imaging Biol 2003;5:42–48. [PubMed: 14499161]
88. Henze M, Schuhmacher J, Dimitrakopoulou-Strauss A, Strauss LG, Macke HR, Eisenhut M, Haberkorn U. Exceptional increase in somatostatin receptor expression in pancreatic neuroendocrine tumour, visualized with ^{68}Ga-DOTATOC PET. Eur J Nucl Med Mol Imaging 2004;31:466. [PubMed: 14730407]
89. Koukouraki, S.; Strauss, LG.; Georgoulias, V.; Schuhmacher, J.; Haberkorn, U.; Karkavitsas, N.; Dimitrakopoulou-Strauss, A. Eur J Nucl Med Mol Imaging. Vol. 33. 2006. Evaluation of the pharmacokinetics of ^{68}Ga-DOTATOC in patients with metastatic neuroendocrine tumours scheduled for ^{90}Y-DOTATOC therapy; p. 460-466.
90. Henze M, Dimitrakopoulou-Strauss A, Milker-Zabel S, Schuhmacher J, Strauss LG, Doll J, et al. Characterization of (^{68}Ga)-DOTA-D-Phe1-Tyr3-octreotide (DOTATOC) kinetics in patients with meningiomas. J Nucl Med 2005;46:763–769. [PubMed: 15872348]
91. Koukouraki S, Strauss LG, Georgoulias V, Eisenhut M, Haberkorn U, Dimitrakopoulou-Strauss A. Comparison of the pharmacokinetics of ^{68}Ga-DOTATOC and [^{18}F]FDG in patients with metastatic neuroendocrine tumours scheduled for ^{90}Y-DOTATOC therapy. Eur J Nucl Med Mol Imaging 2006;33:1115–1122. [PubMed: 16763820]
92. Liu S. Bifunctional coupling agents for target-specific delivery of metallic radionuclides. Advanced Drug Delivery Reviews 2008;60:1347–1370. [PubMed: 18538888]
93. Liu S. HYNIC derivatives as bifunctional coupling agents for ^{99m}Tc-labeling of small biomolecules. Topics in Current Chem 2005;252:193–216.
94. André J, Maecke H, Zehnder M, Macko L, Akyel K. 1,4,7-triazanonane-1-succinic acid-4,7-diacetic acid (NODASA): a new bifunctional chelator for radio gallium-labeling of biomolecules. Chem Commun 1998;12:1301–1302.
95. Eisenwiener KP, Prata MI, Buschmann I, Zhang HW, Santos AC, Wenger S, Reubi JC, Maecke HR. NODAGATOC, a new chelator-coupled somatostatin analogue labeled with [^{67}Ga/^{68}Ga] and [^{111}In] for SPECT, PET, and targeted therapeutic applications of somatostatin receptor ($hsst_2$) expressing tumors. Bioconj Chem 2002;13:530–541.
96. Eisenwiener KP, Powell P, Maecke HR. A convenient synthesis of novel bifunctional pro-chelators for coupling to bioactive peptides for radiometal labeling. Bioorg Med Chem Lett 2000;10:2133–2135. [PubMed: 10999487]
97. McQuade P, Miao Y, Yoo J, Quinn TP, Welch MJ, Lewis JS. Imaging of melanoma using ^{64}Cu- and ^{86}Y-DOTA-ReCCMSH(Arg^{11}), a cyclized peptide analogue of α-MSH. J Med Chem 2005;48:2985–2992. [PubMed: 15828837]
98. Prasanphanich AF, Nanda PK, Rold TL, Ma L, Lewis MJ, Garrison JC, Hoffman TJ, Sieckman GL, Figueroa SD, Smith CJ. [^{64}Cu-NOTA-8-Aoc-BBN(7-14)NH_2] targeting vector for positron-emission tomography imaging of gastrin-releasing peptide receptor-expressing tissues. PNAS 2007;104:12462–12467. [PubMed: 17626788]
99. Harris TD, Kalogeropoulos S, Nguyen T, Liu S, Bartis J, Ellars CE, Edwards DS, Onthank D, Yalamanchili P, Robinson SP, Lazewatsky J, Barrett JA, Bozarth J. Design, synthesis and evaluation of radiolabeled integrin $\alpha_v\beta_3$ receptor antagonists for tumor imaging and radiotherapy. Cancer Biother Radiopharm 2003;18:627–641. [PubMed: 14503959]
100. Onthank DC, Liu S, Silva PJ, Barrett JA, Harris TD, Robinson SP, Edwards DS. ^{90}Y and ^{111}In complexes of A DOTA-conjugated integrin $\alpha_v\beta_3$ receptor antagonist: different but biologically equivalent. Bioconj Chem 2004;15:235–241.
101. Harris TD, Cheesman E, Harris AR, Sachleben R, Edwards DS, Liu S, Bartis J, Ellars C, Onthank D, Yalamanchili P, Heminway S, Silva P, Robinson S, Lazewatsky J, Rajopadhye M, Barrett JA. Radiolabeled divalent peptidomimetic vitronectin receptor antagonists as potential tumor radiotherapeutic and imaging Agents. Bioconj Chem 2007;18:1266–1279.

102. Harris TD, Kalogeropoulos S, Nguyen T, Dwyer G, Edwards DS, Liu S, Bartis J, Ellars C, Onthank D, Yalamanchili P, Heminway S, Robinson S, Lazewatsky J, Barrett J. Structure-Activity relationships of ^{111}In- and ^{99m}Tc-labeled quinolin-4-one peptidomimetics as ligands for the vitronectin receptor: potential tumor imaging agents. Bioconj Chem 2006;17:1294–1313.

103. Chen X, Sievers E, Hou Y, Park R, Tohme M, Bart R, Bremner R, Bading JR, Conti PS. Integrin $\alpha_v\beta_3$–targeted imaging of lung cancer. Neoplasia 2005;7:271–279. [PubMed: 15799827]

104. Morrison MS, Ricketts SA, Barnett J, Cuthbertson A, Tessier J, Wedge SR. Use of a novel Arg-Gly-Asp radioligand, ^{18}F-AH111585, to determine changes in tumor vascularity after antitumor therapy. J Nucl Med 2009;50:116–122. [PubMed: 19091899]

105. Kenny LM, Coombes RC, Oulie I, Contractor KB, Miller M, Spinks TJ, McParland B, Cohen PS, Hui A, Palmieri C, Osman S, Glaser M, Turton D, Al-Nahhas A, Aboagye EO. Phase I trial of the positron-emitting Arg-Gly-Asp (RGD) peptide radioligand ^{18}F-AH111585 in breast cancer patients. J Nucl Med 2008;49:879–886. [PubMed: 18483090]

106. Beer AJ, Haubner R, Goebel M, Luderschmidt S, Spilker ME, Wester HJ, Weber WA, Schwaiger M. Biodistribution and pharmacokinetics of the $\alpha_v\beta_3$-selective tracer ^{18}F-Galacto-RGD in cancer patients. J Nucl Med 2005;46:1333–1341. [PubMed: 16085591]

107. Haubner R, Weber WA, Beer AJ, Vabulience E, Reim D, Sarbia M, Becker KF, Goebel M, Hein R, Wester HJ, Kessler H, Schwaiger M. Noninvasive visualization of the activiated $\alpha_v\beta_3$ integrin in cancer patients by positron emission tomography and [^{18}F]Galacto-RGD. PLOS Medicine 2005;2:e70, 244–252. [PubMed: 15783258]

108. Beer AJ, Grosu AL, Carlsen J, Kolk A, Sarbia M, Stangier I, Watzlowik P, Wester HJ, Haubner R, Schwaiger M. [^{18}F]Galacto-RGD positron emission tomography for imaging of $\alpha_v\beta_3$ expression on the neovasculature in patients with squamous cell carcinoma of the head and neck. Clin Cancer Res 2007;13:6610–6616. [PubMed: 18006761]

109. Beer AJ, Niemeyer M, Carlsen J, Sarbia M, Nahrig J, Watzlowik P, Wester HJ, Harbeck N, Schwaiger M. Patterns of alphavbeta3 expression in primary and metastatic human breast cancer as shown by ^{18}F-Galacto-RGD PET. J Nucl Med 2008;49:255–259. [PubMed: 18199623]

110. Haubner R, Finsinger D, Kessler H. Stereoisomeric peptide libraries and peptidomimetics for designing selective inhibitors of the $\alpha_v\beta_3$ integrin for a new cancer therapy. Angew Chem Int Ed Engl 1997;36:1375–1389.

111. Haubner R, Gratias R, Diefenbach B, Goodman SL, Jonczyk A, Kessler H. Structural and functional aspect of RGD-containing cyclic pentapeptides as highly potent and selective integrin $\alpha_v\beta_3$ antagonists. J Am Chem Soc 1996;118:7461–7472.

112. Aumailley M, Gurrath M, Müller G, Calvete J, Timpl R, Kessler H. Arg-Gly-Asp constrained within cyclic pentapeptides strong and selective inhibitors of cell adhesion to vitronectin and laminin fragment P1. FEBS Lett 1991;291:50–54. [PubMed: 1718779]

113. Gottschalk KE, Kessler H. The structures of integrins and integrin-ligand complexes: Implications for drug design and signal transduction. Angew Chem Int Ed Engl 2002;41:3767–3774. [PubMed: 12386845]

114. Rajopadhye M, Harris AR, Nguyen HM, Overoye KL, Bartis J, Liu S, Edwards DS, Barrett JA. RP593, a ^{99m}Tc-labeled $\alpha_v\beta_3/\alpha_v\beta_5$ antagonist, rapidly detects spontaneous tumors in mice and dogs. 47th Annual Meeting of SNM, St Louis, Missouri. J Nucl Med 2000;41:34P.

115. Liu S, Edwards DS, Ziegler MC, Harris AR, Hemingway SJ, Barrett JA. ^{99m}Tc-Labeling of a hydrazinonicotinamide-conjugated vitronectin receptor antagonist useful for imaging tumor. Bioconj Chem 2001;12:624–629.

116. Boturyn D, Coll JL, Garanger E, Favrot MC, Dumy P. Template assembled cyclopeptides as multimeric system for integrin targeting and endocytosis. J Am Chem Soc 2004;126:5730–5739. [PubMed: 15125666]

117. Li Z, Cai W, Cao Q, Chen K, Wu Z, Chen X. ^{64}Cu-Labeled tetrameric and octameric RGD peptides for small-animal PET of tumor $\alpha_v\beta_3$ integrin expression. J Nucl Med 2007;48:1162–1171. [PubMed: 17574975]

118. Wang L, Kim YS, Shi J, Zhai S, Jia B, Liu Z, Zhao H, Wang F, Chen X, Liu S. Improving tumor targeting capability and pharmacokinetics of ^{99m}Tc-labeled cyclic RGD dimers with PEG_4 linkers. Mol Pharm 2009;6:231–245. [PubMed: 19067525]

119. Shi J, Wang L, Kim YS, Zhai S, Liu Z, Chen X, Liu S. Improving tumor uptake and excretion kinetics of ^{99m}Tc-labeled cyclic Arginine-Glycine-Aspartic (RGD) dimers with triglycine linkers. J Med Chem 2008;51:7980–7990. [PubMed: 19049428]

120. Cai W, Rao J, Gambhir SS, Chen X. How molecular imaging is speeding up antiangiogenic drug development? Mol Cancer Ther 2006;5:2624–2633. [PubMed: 17121909]

121. Niu G, Chen X. Has molecular and cellular imaging enhanced drug discovery and drug development? Drugs in R&D 2008;9:351–368.

122. Jain RK. Transport of molecules in the tumor interstitium: a review. Cancer Res 1987;47:3039–3051. [PubMed: 3555767]

123. Shi J, Wang L, Kim YS, Zhai S, Liu Z, Chen X, Liu S. Improving tumor uptake and pharmacokinetics of ^{64}Cu-labeled cyclic RGD dimers with triglycine and PEG_4 Linkers. Bioconj Chem 2009;20:750–759.

124. Shi J, Kim YS, Chakraborty S, Zhou Y, Wang F, Liu S. Novel ^{111}In-labeled cyclic RGD peptide dimers: improving tumor uptake and pharmacokinetics with G_3 and PEG_4 Linkers. Dalton Trans. Submitted.

125. Liu Z, Niu G, Shi J, Liu SL, Wang F, Liu S, Chen X. ^{68}Ga-Labeled cyclic RGD dimers with Gly_3 and PEG_4 linkers: promising agents for tumor integrin $\alpha_v\beta_3$ PET imaging. Eur J Nucl Med Mol Imaging 2009;36:947–957. [PubMed: 19159928]

126. Liu Z, Liu S, Wang F, Liu S, Chen X. Non-invasive imaging of tumor integrin expression using ^{18}F-labeled RGD dimer peptide with PEG_4 linkers. Eur J Nucl Med Mol Imaging ASAP. 2009

127. Fani M, Andre JP, Maecke HR. ^{68}Ga-PET: a powerful generator-based alternative to cyclotron-based PET radiopharmaceuticals. Contrast Media Mol Imaging 2008;3:53–63. [PubMed: 18383455]

128. Maecke HR, Andre JP. ^{68}Ga-PET radiopharmacy: A generator-based alternative to ^{18}F-radiopharmacy. Ernst Schering Res Found Workshop 2007;62:215–242. [PubMed: 17172157]

129. Al-Nahhas A, Win Z, Szyszko T, Singh A, Khan S, Rubello D. What can gallium-68 PET add to receptor and molecular imaging? Eur J Nucl Med Mol Imaging 2007;34:1897–1901. [PubMed: 17713764]

130. Creamer D, Allen M, Sousa A, Poston R, Barker J. Altered vascular endothelium integrin expression in psoriasis. Am J Pathol 1995;147:1661–1667. [PubMed: 7495291]

131. Waldeck J, Häger F, Höltke C, Lanckohr C, von Wallbrunn A, Torsello G, Heindel W, Theilmeier G, Schäfers M, Bremer C. Fluorescent reflectance imaging of macrophage-rich atherosclerostic plaques using $\alpha_v\beta_3$ integrin-targeted fluorochrome. J Nucl Med 2008;49:1845–1851. [PubMed: 18927332]

132. Meoli DF, Sadeghi MM, Krassilnikova S, Bourke BN, Giordano FJ, Dione DP, Su HL, Edwards DS, Liu S, Harris TD, Madri JA, Zaret BL, Sinusas AJ. Noninvasive imaging of myocardial angiogenesis following experimental myocardial infarction. J Clin Invest 2004;113:1684–1691. [PubMed: 15199403]

133. Pichler BJ, Kneilling M, Haubner R, Braumüller H, Schwaiger M, Röcken M, Weber WA. Imaging of delayed-type hypersensitivity reaction by PET and ^{18}F-Galacto-RGD. J Nucl Med 2005;46:184–189. [PubMed: 15632051]

134. Hua J, Dobrucki LW, Sadeghi MM, Zhang J, Bourke BN, Cavaliere P, Song J, Chow C, Jahanshad N, van Royen N, Buschmann I, Madri JA, Mendizabal M, Sinusas A. Noninvasive imaging of angiogenesis with a ^{99m}Tc labeled peptide targeted at $\alpha_v\beta_3$ integrin after murine hindlimb ischemia. Circulation 2005;111:3255–3260. [PubMed: 15956134]

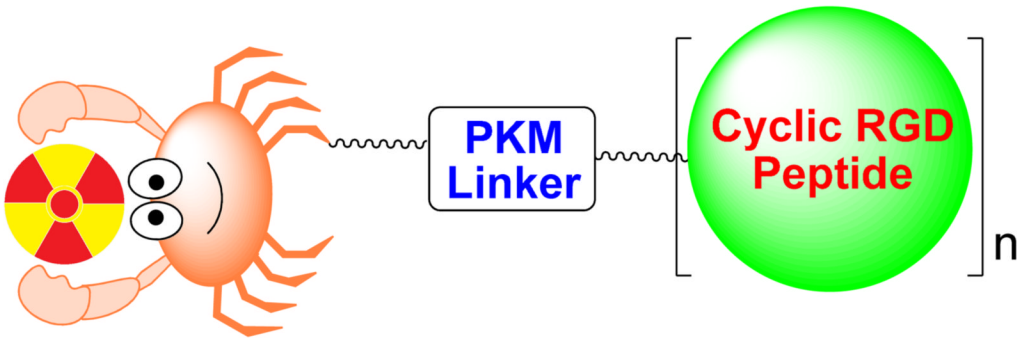

Figure 1.
Schematic presentation of the radiotracer design. The targeting biomolecule is a multimeric cyclic RGD peptide. The PKM linker is used to modify radiotracer pharmacokinetics. For the metal-containing radiotracers, a multidentate BFC is often used to attach the metallic radionuclide to the targeting biomolecule. For ^{18}F-based radiotracers, an organic precursor or synthon is often needed to attach ^{18}F onto the multimeric cyclic RGD peptide.

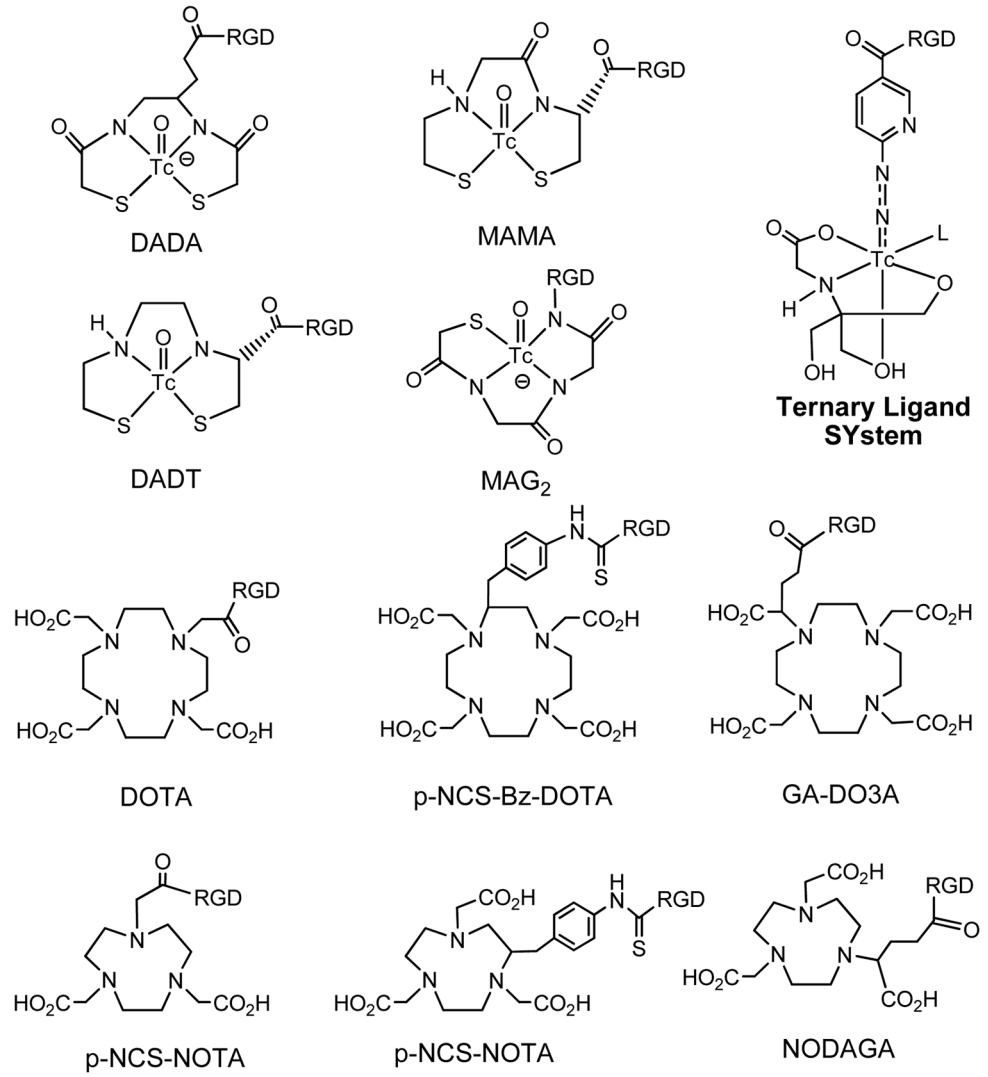

Figure 2.

BFCs useful for radiolabeling of multimeric cyclic RGD peptides with ^{99m}Tc, ^{68}Ga and ^{64}Cu. DADA (diamidodithiol), MAMA (monoaminemonoamidedithiol), MADT (diaminedithiol), MAG_2 (2-mecaptoacetylglycylglycyl) and HYNIC are particularly useful for ^{99m}Tc-labeling while DOTA, NOTA and their derivatives are excellent BFCs for chelation of ^{68}Ga and ^{64}Cu.

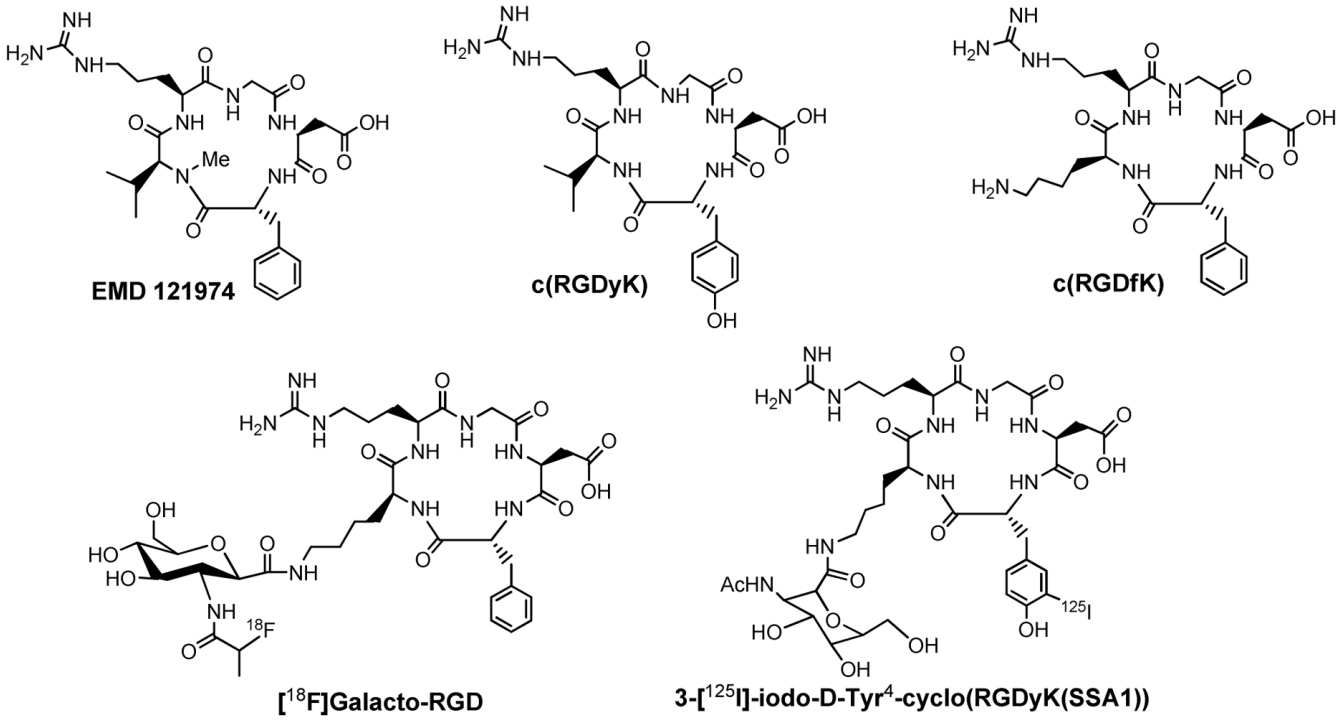

Figure 3.

Chemdraw structures of cyclic RGD peptides useful as targeting biomolecules for the integrin $\alpha_v\beta_3$-targeted radiotracers. [^{18}F]Galacto-RGD (2-[^{18}F]fluoropropanamide c(RGDfK(SAA); SAA = 7-amino-L-glyero-L-galacto-2,6-anhydro-7-deoxyheptanamide) is currently under clinical investigation for visualization of integrin $\alpha_v\beta_3$ expression in cancer patients

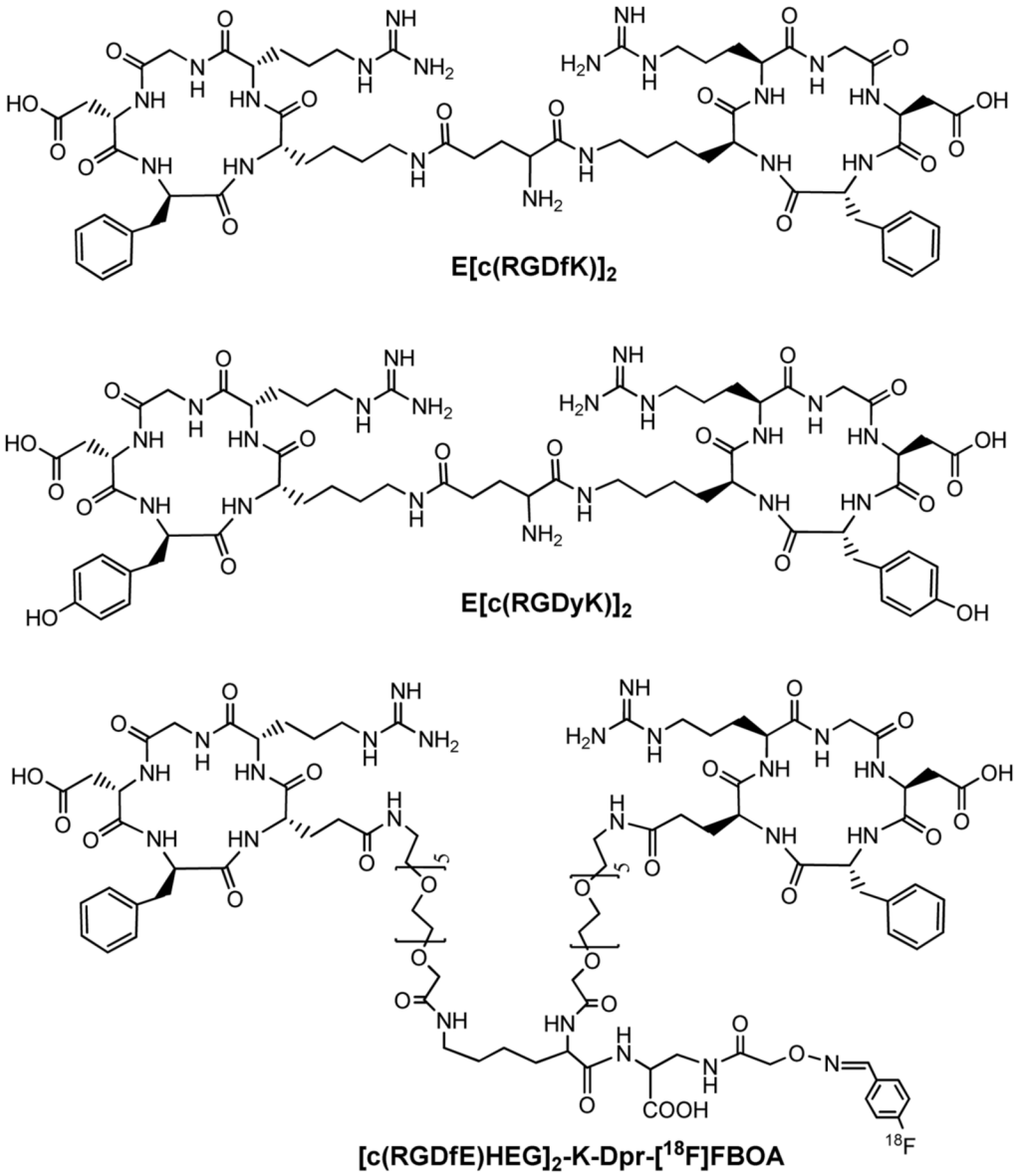

Figure 4.
Cyclic RGD peptide dimers (E[c(RGDfK)]$_2$ and E[c(RGDyK)]$_2$) and [c(RGDfE)HEG]$_2$-K-Dpr-[^{18}F]FBOA.

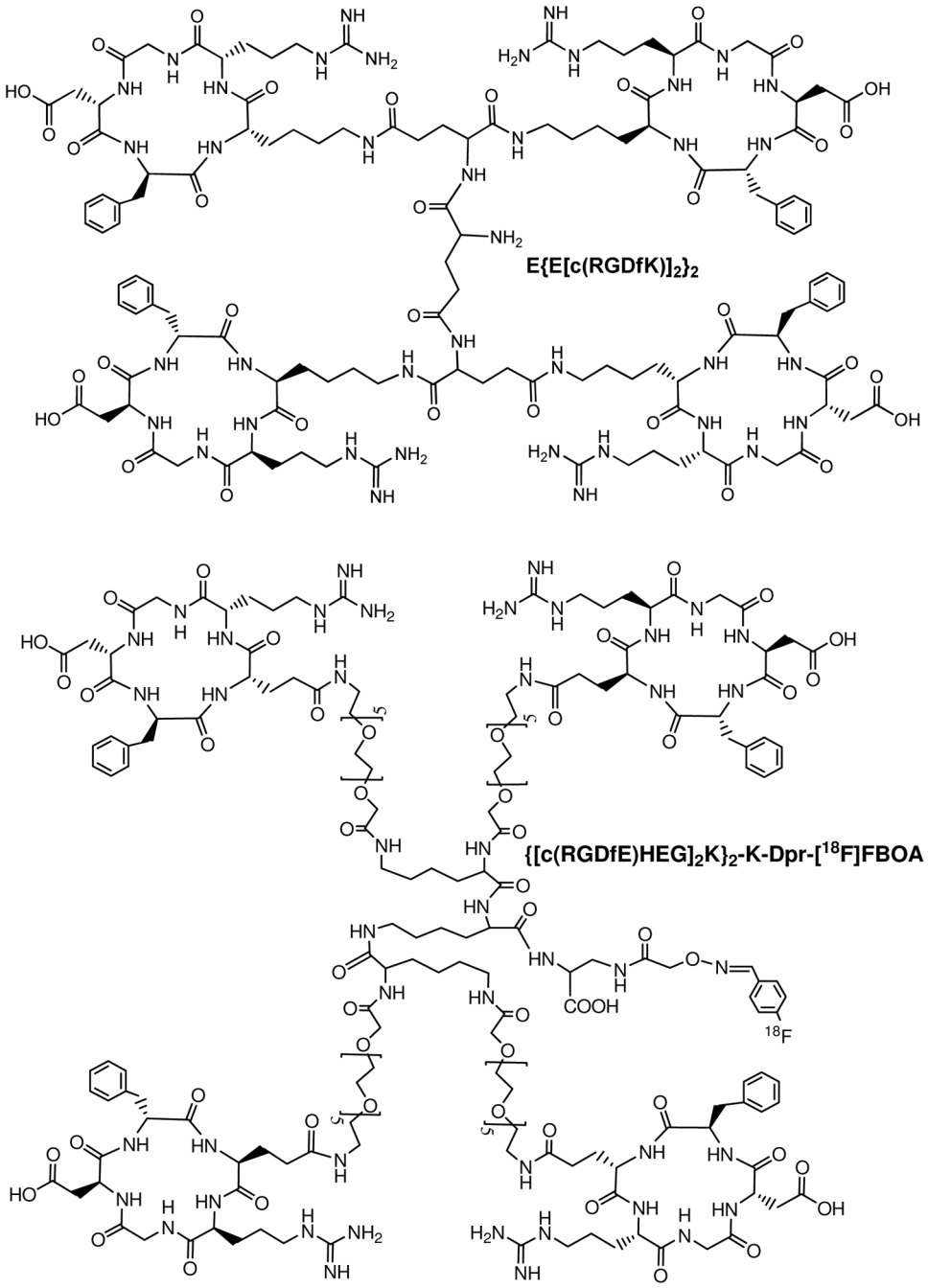

Figure 5.
A cyclic RGDfK peptide tetramer, $E\{E[c(RGDfK)]_2\}_2$ and a ^{18}F-labeled cyclic RGDfE tetramer, $\{[c(RGDfE)HEG]_2K\}_2$-K-Dpr-[^{18}F]FBOA.

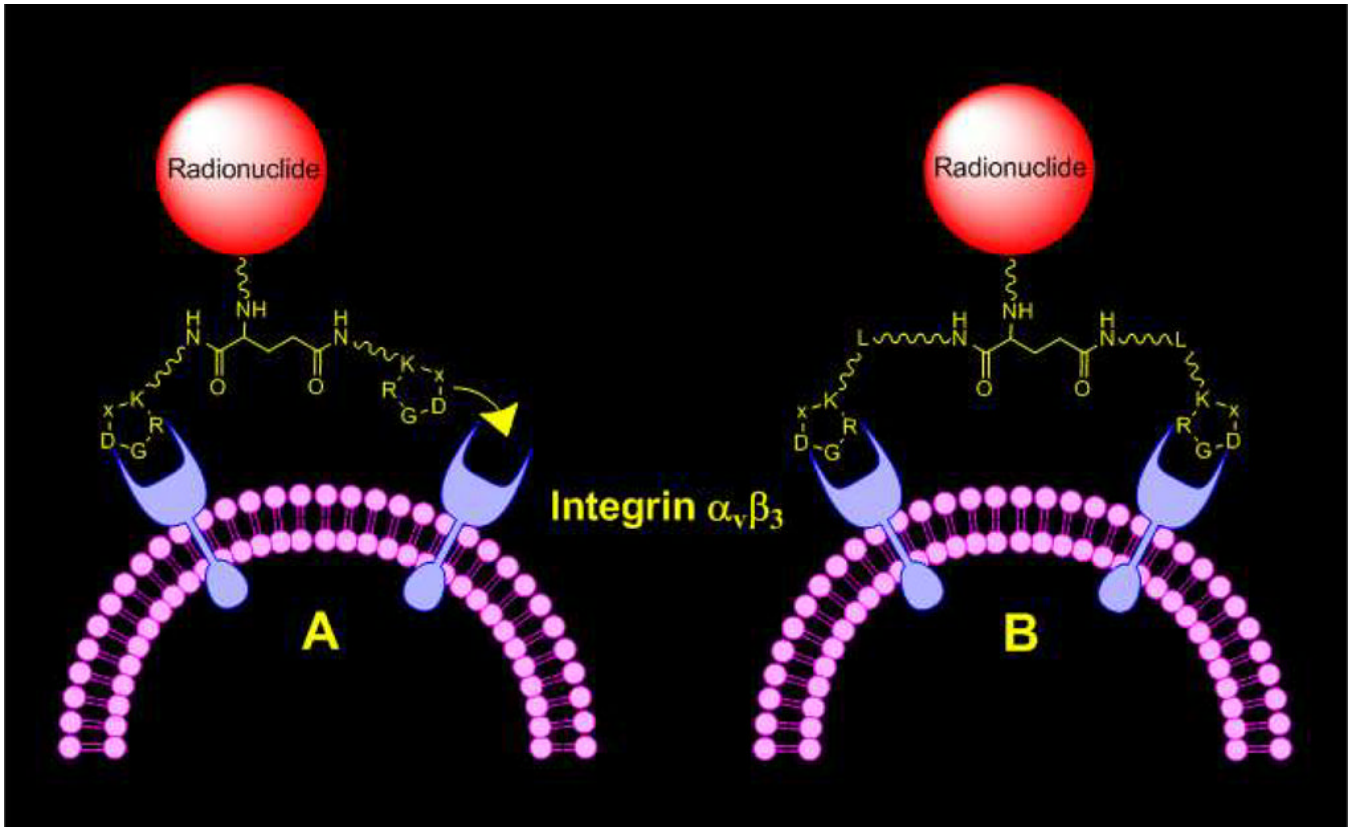

Figure 6.

Schematic illustration of interactions between cyclic RGD peptide dimers and integrin $\alpha_v\beta_3$. **A**: The distance between two RGD motifs is not long enough for simultaneous integrin $\alpha_v\beta_3$ binding. However, the RGD concentration is "locally enriched" in the vicinity of neighboring integrin $\alpha_v\beta_3$ once the first RGD motif is bound. **B**: The distance between two RGD motifs is long due to the presence of two linkers (L). As a result, the cyclic RGD dimer is able to bind integrin $\alpha_v\beta_3$ in a "bivalent" fashion. In both cases, the end-result would be higher integrin $\alpha_v\beta_3$ binding affinity for the multimeric cyclic RGD peptides.

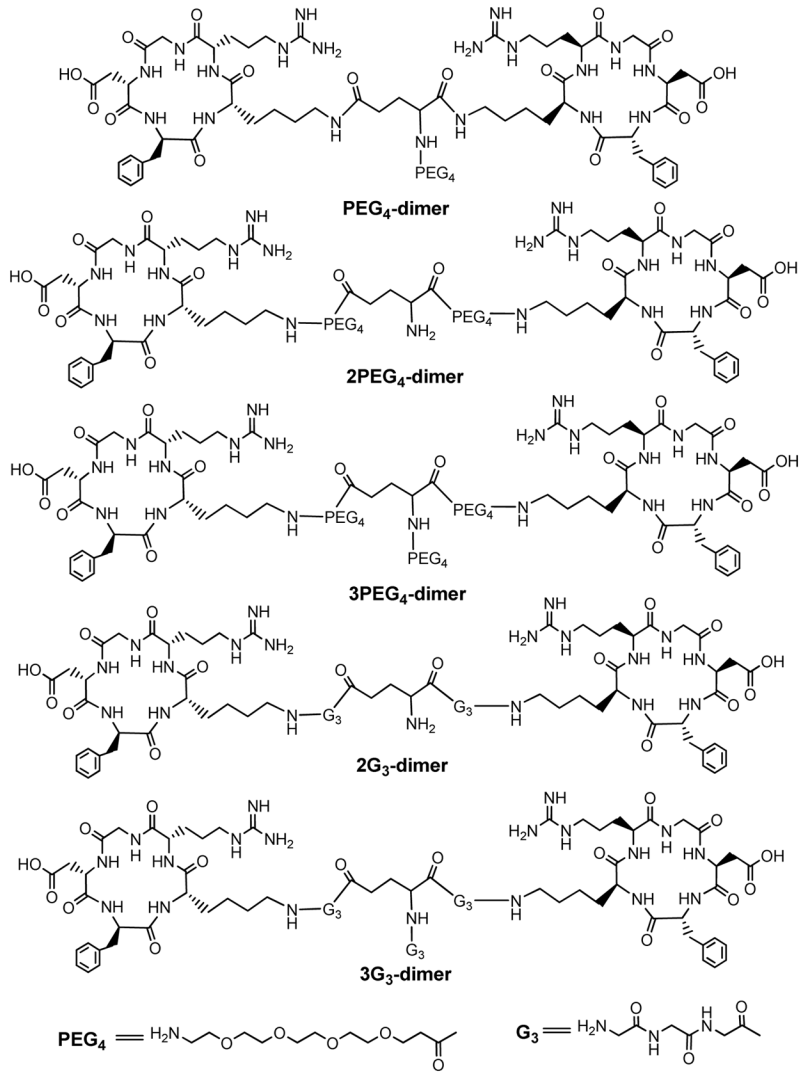

Figure 7.

New cyclic RGD peptide dimers useful for the development of integrin $\alpha_v\beta_3$–targeted radiotracers. The PEG_4 and G_3 linkers are used to increase the distance between two RGD motifs and to improve radiotracer excretion kinetics from non-cancerous organs.

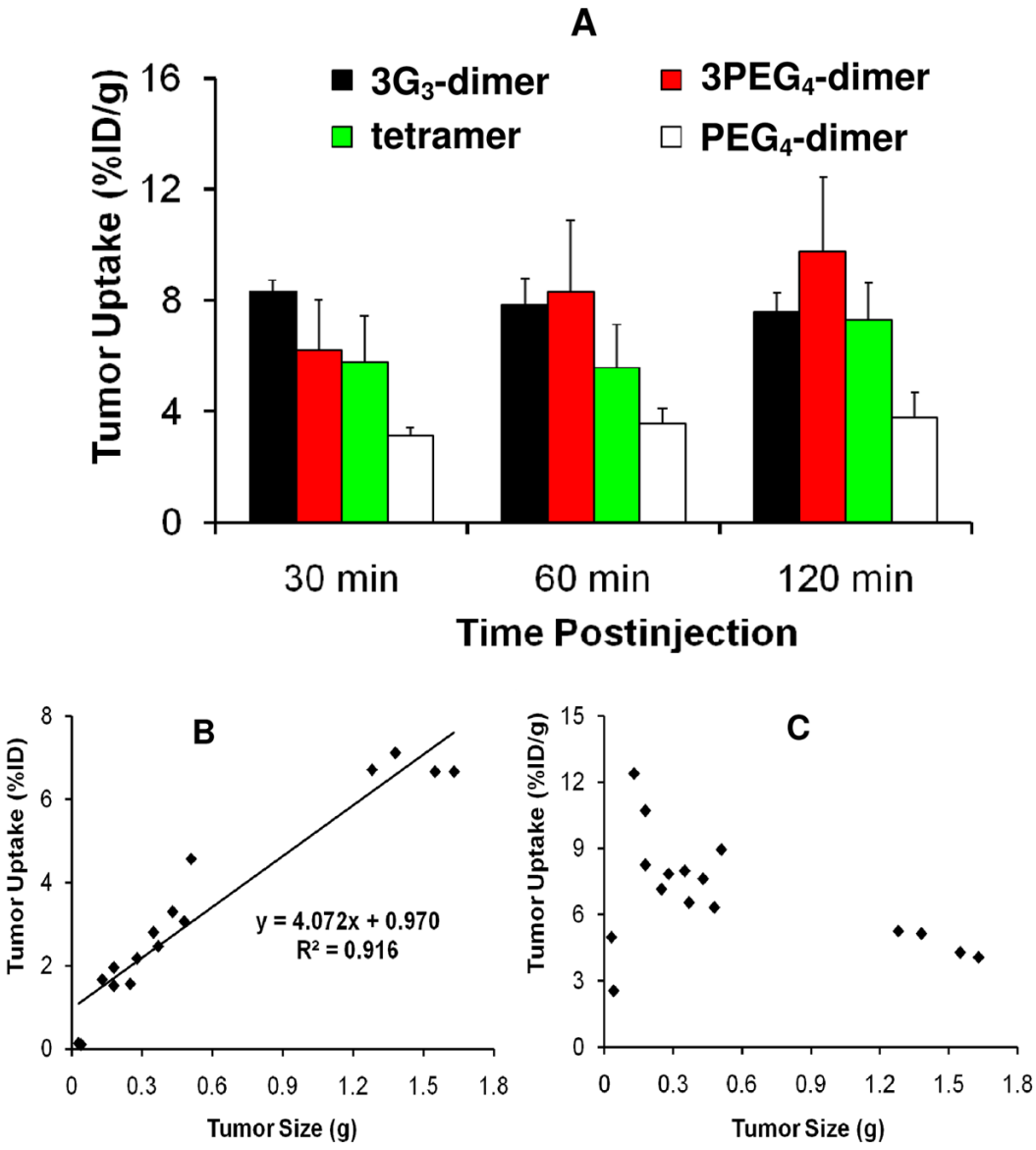

Figure 8.

Top: direct comparison of the tumor uptake for ^{99m}Tc-PEG$_4$-dimer, ^{99m}Tc-3G$_3$-dimer, ^{99m}Tc-3PEG$_4$-dimer and ^{99m}Tc-tetramer in athymic nude mice bearing MDA-MB-435 breast cancer xenografts (**A**). Bottom: the relationship between the tumor size and tumor uptake (**B** and **C**) of ^{99m}Tc-3PEG$_4$-dimer at 120 min p.i. in athymic nude mice bearing U87MG glioma xenografts. The linear relationship suggests that ^{99m}Tc-3PEG$_4$-dimer is for monitoring the tumor growth or shrinkage during anti-angiogenic therapy.

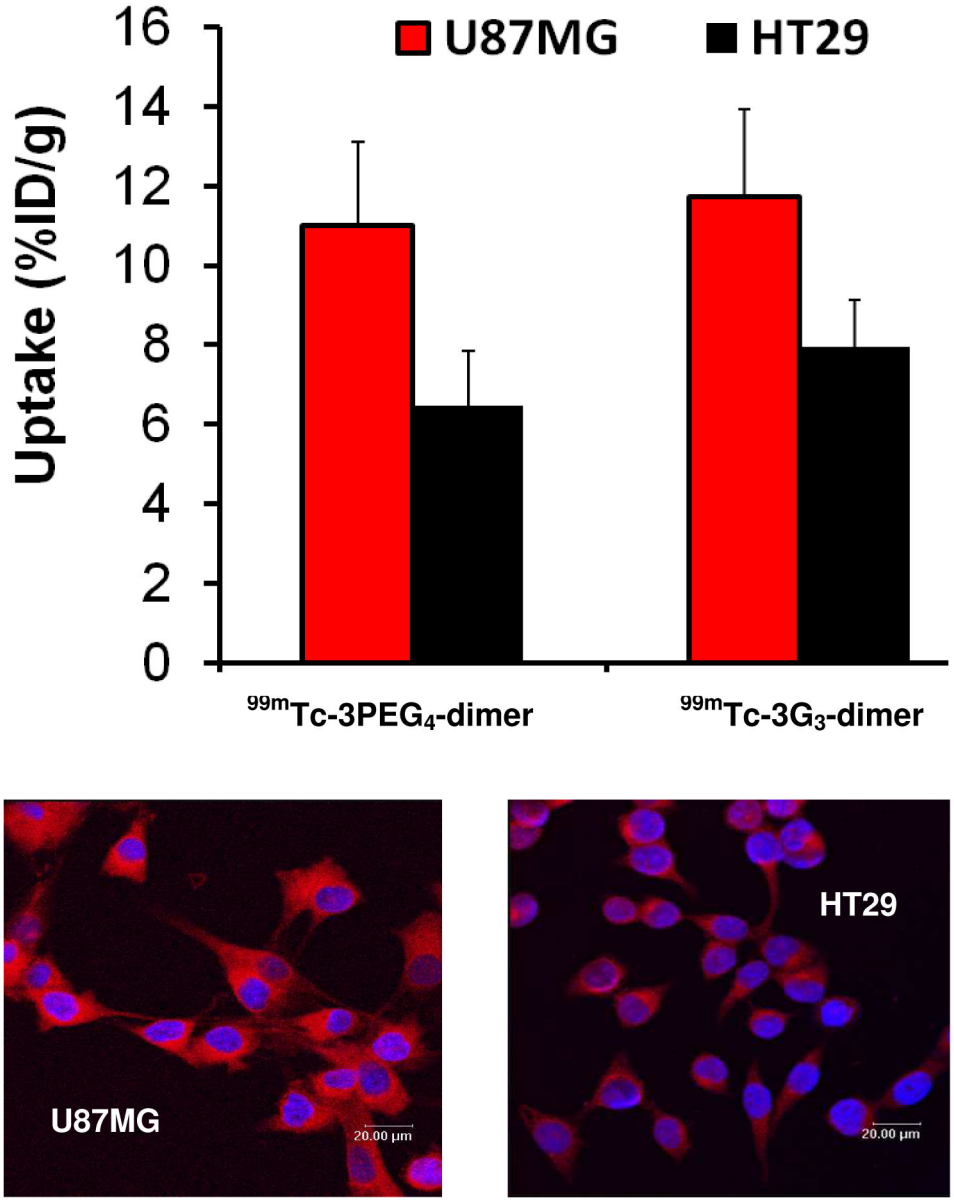

Figure 9.

Top: direct comparison of the tumor uptake for ^{99m}Tc-3PEG$_4$-dimer and ^{99m}Tc-3G$_3$-dimer in athymic nude mice bearing U87MG glioma and HT29 colon cancer xenografts. Bottom: confocal microscope images of U87MG glioma (left) and HT29 (right) tumor cells. The blue color indicates the presence cell nuclei (the presence of 4′,6′-diamidino-2-phenylindole). The red color indicates the presence of integrin $\alpha_v\beta_3$ due to the binding of LM609 and TRITC-coupled goat-anti-mouse IgG. These data show that the integrin $\alpha_v\beta_3$ level on tumor cells (U87MG > HT29) plays a significant role in the radiotracer tumor uptake.

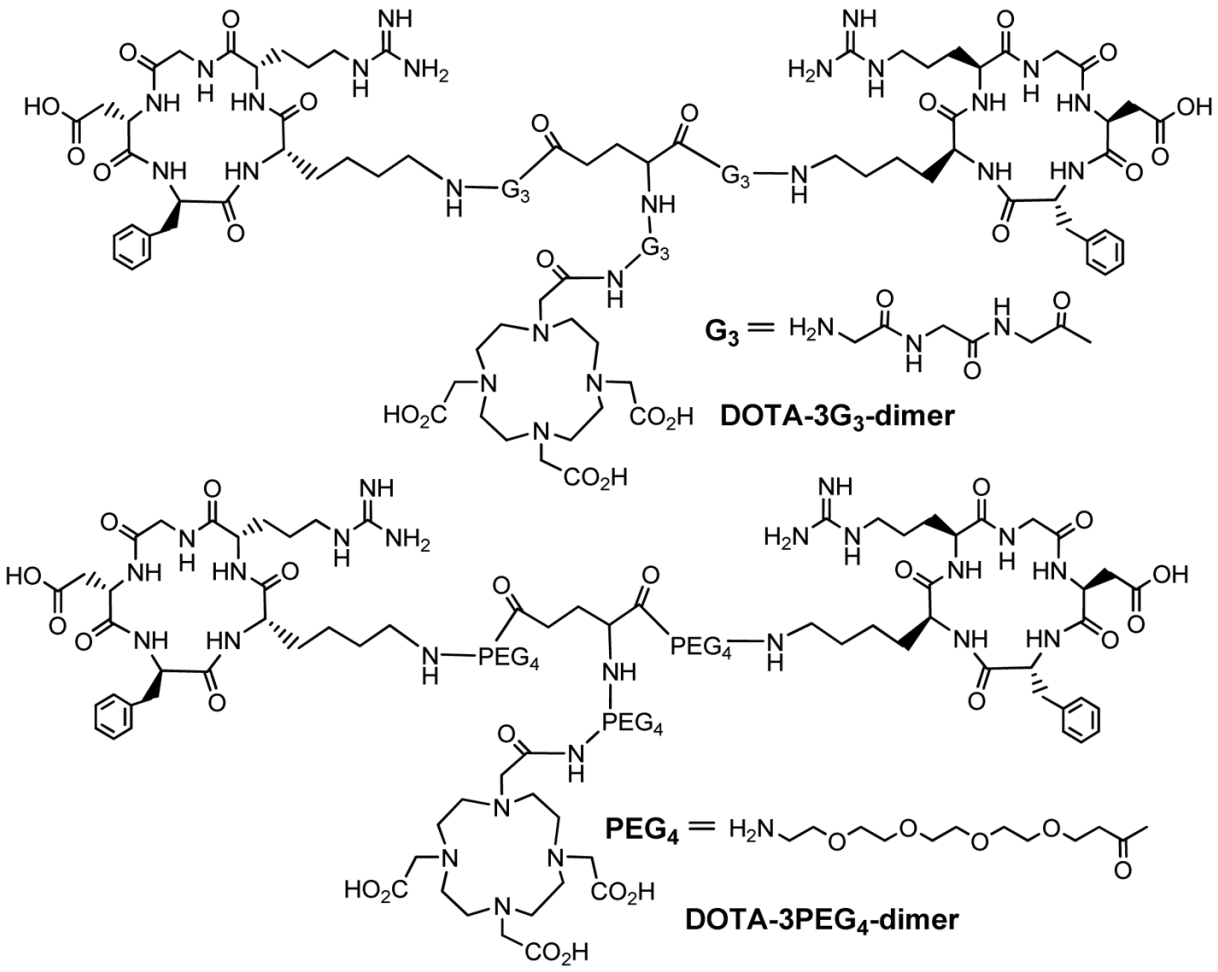

Figure 10.
Structures of DOTA-3G_3-dimer and DOTA-3PEG_4-dimer.

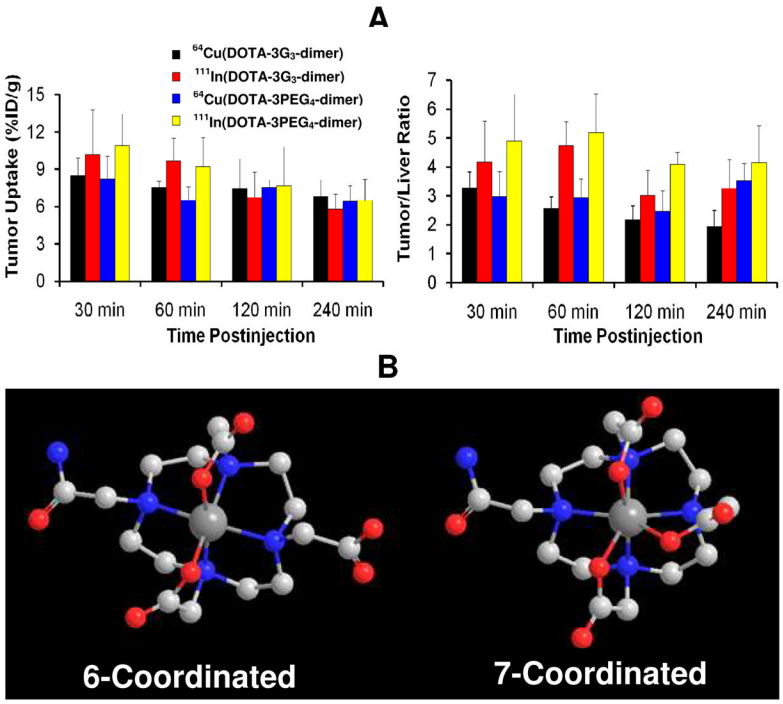

Figure 11.

A: comparison of tumor uptake and tumor/liver ratios for ^{64}Cu(DOTA-3PEG$_4$-dimer), ^{64}Cu(DOTA-3G$_3$-dimer), ^{111}In(DOTA-3PEG$_4$-dimer) and ^{111}In(DOTA-3G$_3$-dimer) in athymic nude mice bearing U87MG human glioma xenografts. **B**: Chem-3D presentation of ^{64}Cu(DOTA-monoamide) (6-coordinated) and ^{111}In(DOTA-monoamide) (7-coordinated).

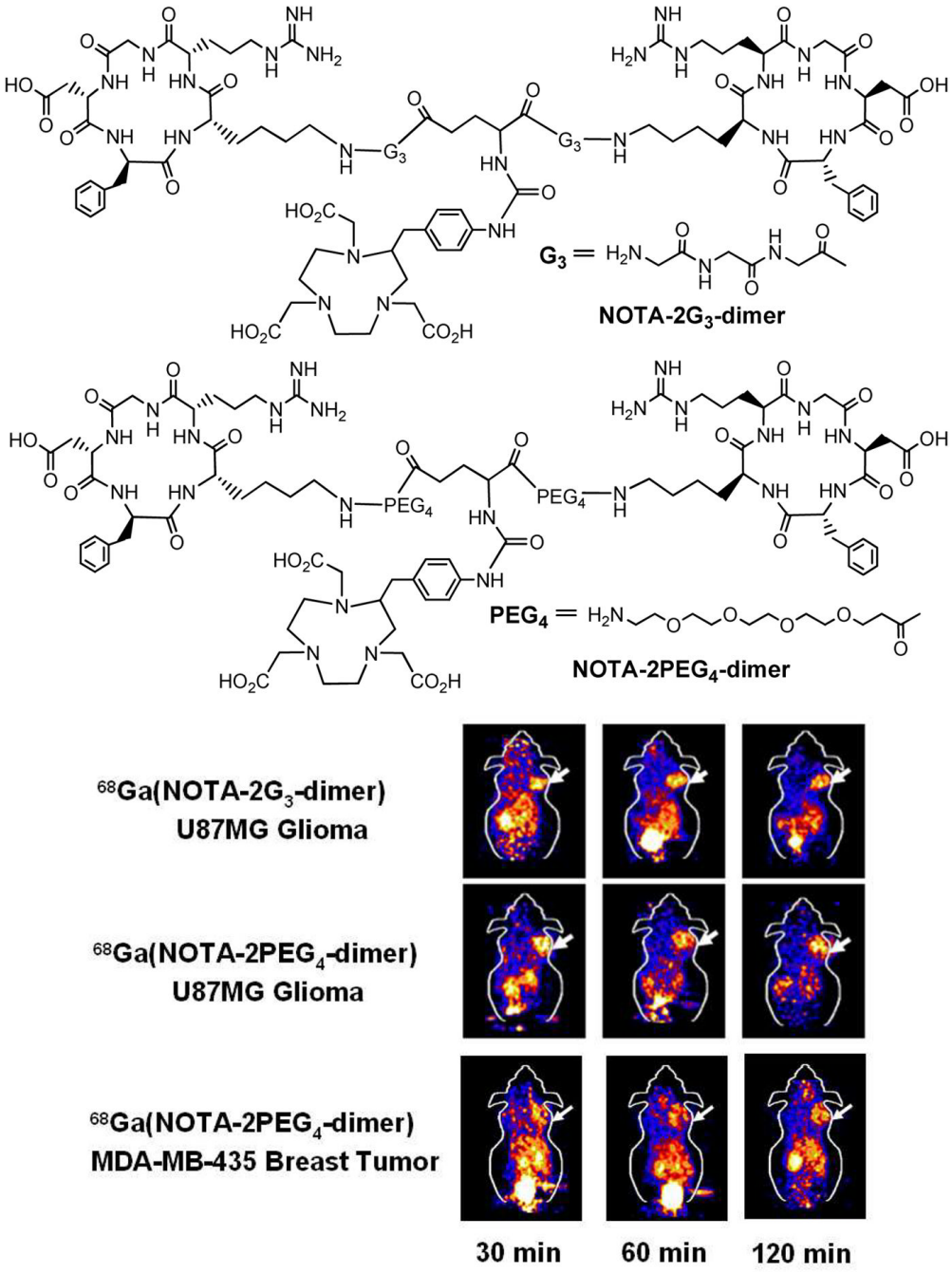

Figure 12.

Top: structures of NOTA-2G_3-dimer and NOTA-2PEG_4-dimer. Bottom: microPET images for ^{68}Ga(NOTA-2G_3-dimer) and ^{68}Ga(NOTA-2PEG_4-dimer). Arrows indicate the presence of tumors.

Table 1

Integrin $\alpha_v\beta_3$ binding data for HYNIC-conjugated cyclic RGD peptides against ^{125}I-echistatin bound to the integrin $\alpha_v\beta_3$–positive U87MG human glioma cells.

Compound	Radiotracer	IC_{50} (nM)
HYNIC-G_3-monomer	[^{99m}Tc(HYNIC-G_3-monomer)(tricine)(TPPTS)]	358 ± 8
HYNIC-PEG_4-monomer	[^{99m}Tc(HYNIC-PEG_4-monomer)(tricine)(TPPTS)]	452 ± 11
HYNIC-dimer	[^{99m}Tc(HYNIC-dimer)(tricine)(TPPTS)]	112 ± 21
HYNIC-PEG_4-dimer	[^{99m}Tc(HYNIC-PEG_4-dimer)(tricine)(TPPTS)]	84 ± 7
HYNIC-2G_3-dimer	[^{99m}Tc(HYNIC-2G_3-dimer)(tricine)(TPPTS)]	60 ± 4
HYNIC-2PEG_4-dimer	[^{99m}Tc(HYNIC-2PEG_4-dimer)(tricine)(TPPTS)]	52 ± 7
HYNIC-3G_3-dimer	[^{99m}Tc(HYNIC-3G_3-dimer)(tricine)(TPPTS)]	61 ± 2
HYNIC-3PEG_4-dimer	[^{99m}Tc(HYNIC-3PEG_4-dimer)(tricine)(TPPTS)]	62 ± 5
HYNIC-tetramer	[^{99m}Tc(HYNIC-dimer)(tricine)(TPPTS)]	7 ± 2
DOTA-dimer	^{64}Cu(DOTA-dimer)/^{111}In(DOTA-dimer)	102 ± 5
DOTA-3G_3-dimer	^{64}Cu(DOTA-3G_3-dimer)/^{111}In(DOTA-3G_3-dimer)	74 ± 3
DOTA-3PEG_4-dimer	^{64}Cu(DOTA-3PEG_4-dimer)/^{111}In(DOTA-3PEG_4-dimer)	62 ± 6
DOTA-tetramer	^{64}Cu(DOTA-tetramer)/^{111}In(DOTA-tetramer)	10 ± 2
NOTA-dimer	^{68}Ga(NOTA-dimer)	100 ± 3
NOTA-2G_3-dimer	^{68}Ga(NOTA-2G_3-dimer)	66 ± 4
NOTA-3PEG_4-dimer	^{68}Ga(NOTA-2PEG_4-dimer)	54 ± 2